Green Chemistry

ROYAL SOCIETY OF CHEMISTRY

TUTORIAL REVIEW

View Article Online
View Journal | View Issue

Cite this: *Green Chem.*, 2024, **26**, 10774

Biodegradable polymers: from synthesis methods to applications of lignin-*graft*-polyester

Sundol Kim and Hoyong Chung *

The issue of non-degradable petroleum-based plastic waste is a global challenge that requires urgent attention due to its harmful impact on humans and the environment. Biomass-based materials have garnered significant attention to address this challenge in recent times. Lignin, with its abundance, low price, and rich aromatic groups, is not only essential biomass but also a crucial material that can be utilized to produce biodegradable polymers. This review paper provides comprehensive knowledge of the synthesis and applications related to lignin, polyester, and lignin–polyester copolymers with a specific focus on organic polymer synthesis techniques and diverse applications. Beginning with lignin, the review explores various extraction methods from raw biomass resources aimed at enhancing its compatibility with polyester matrices. Next, we discuss lignin chemical modification methods that alter its chemical structure and properties, ultimately enhancing its integration with polyesters. Subsequently, the synthesis of polyester is examined, encompassing condensation polymerizations and ring-opening polymerizations. These methods are evaluated for their scalability and capability in producing tailored polymer chains suitable for copolymerization with lignin. The copolymerization strategies involving lignin and polyester are explored in detail, including graft-onto and graft-from approaches. Each method is discussed for its ability to control copolymer composition and properties, which are crucial for achieving desired material characteristics. In terms of applications, the review highlights the wide-ranging utility of lignin–polyester copolymers across industries such as packaging, construction, and separation. These polymers offer improved biodegradability, thermal stability, and mechanical strength compared to conventional polyesters, making them perfect candidates for novel sustainable materials. Overall, this review provides valuable insights into the synthesis methods and applications of lignin, polyester, and lignin–polyester copolymers offering a comprehensive overview of their potential for addressing environmental concerns and expanding the scope of lignin-derived materials in various industrial applications.

Received 19th July 2024,
Accepted 6th September 2024

DOI: 10.1039/d4gc03558e

rsc.li/greenchem

1. Introduction

Environmental pollution with nondegradable petroleum-based plastic has become a serious global and national-scale problem.[1,2] Discarded plastic contaminates all major ecosystems on Earth, and concerns about its negative impact on wildlife and human health are also increasing.[3] Because of this environmental issue, biomass-based or biodegradable polymers have been reported to solve this environmental problem as well as to decrease the dependence on fossil feedstock.

It is crucial to remember that biomass-based does not mean biodegradable.[4] Fig. 1 shows the material coordinate system of bioplastic.[5,6] The *x*-axis means the presence/absence of biodegradation and the *y*-axis means the origin of raw material, whether it is biomass-based or petroleum-based. Biobased polymers (Fig. 1 top) are a renewable biomass resource leading to sustainable material production, reducing carbon footprint and greenhouse gas emissions.[6,7] Biodegradable polymers (Fig. 1 right) are environmentally friendly materials that decompose without leaving behind fragments or harmful products.[4]

Biodegradability is related to a material's chemical and physical structure, not its raw material origin. Therefore, chemical modifications or additives can affect biodegradability, leading to concerns about the biodegradability of chemically modified natural materials. Thus, biomass-based materials can be non-biodegradable such as bio polyethylene (Bio-PE), bio polyethylene terephthalate (Bio-PET), bio trimethylene terephthalate (Bio-PTT), bio polypropylene (Bio-PP), and bio polyamides (Bio-PA).[8] On the other hand, petroleum-based polymers can be biodegradable polymers such as poly

Department of Chemical and Biomedical Engineering, FAMU-FSU College of Engineering, Tallahassee, FL 32310, USA. E-mail: hchung@eng.famu.fsu.edu

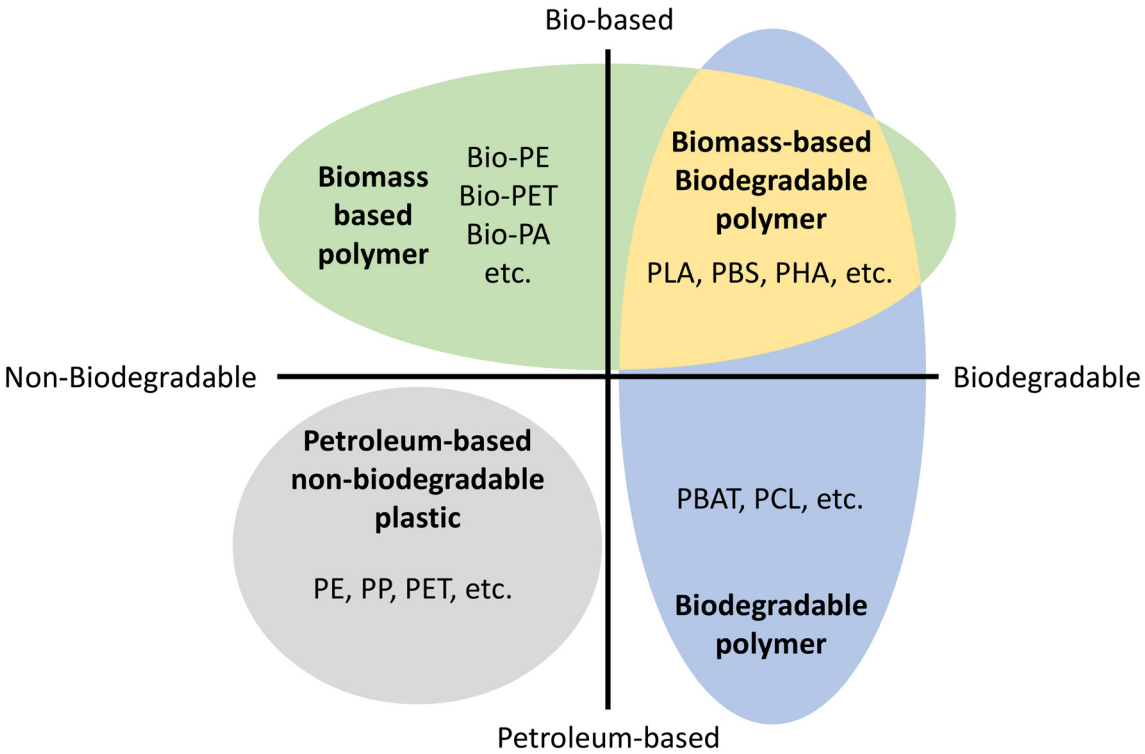

Fig. 1 Material coordinate system of bioplastics.[5,6] Bio-PE: bio polyethylene, Bio-PET: bio poly(ethylene terephthalate), Bio-PA: bio polyamides, PLA: poly(lactic acid). PBS: poly(butylene succinate), PHA: poly(hydroxyalkanoates), PE: polyethylene, PP: polypropylene, PET: poly(ethylene terephthalate), PBAT: poly(butylene adipate terephthalate), PCL: poly(caprolactone).

(caprolactone). As a result, the ultimate and desirable solution to the overall plastic waste problem is biomass-based and biodegradable polymers (Fig. 1 top right).

Biodegradability refers to a material's ability to be broken down by microorganisms, such as bacteria and fungi, into natural substances like water, carbon dioxide, and biomass.[9,10] This process can occur in various environments, including soil, water, and anaerobic conditions, with the rate of biodegradation varying significantly depending on factors such as temperature, humidity, and oxygen availability. Materials that decompose into non-toxic components within a specified period under controlled conditions are especially considered compostable, and the resulting compost can be used to enhance soil health.[9,10]

However, not all biodegradable materials behave the same way in natural environments. This means some plastics are engineered to degrade only under specific conditions, such as elevated temperatures or in the presence of particular microorganisms, which may not be found in nature. For example, polylactic acid (PLA)[10] is a widely used biodegradable plastic, commonly found in packaging and disposable tableware. While PLA is compostable, it typically requires temperatures above 55–60 °C to decompose effectively.[11,12] However, in natural environments such as the ocean or soil, PLA may not decompose as intended. Even when PLA eventually decomposes, it often fragments into microplastics before it fully decomposes. These tiny plastic particles persist in the environment, accumulating in water bodies and ingested by marine life, which can pose a persistent environmental risk.

2. Lignin

Lignin is one of the biopolymers found in the cells of plant species and some algae.[13] It is mainly in the secondary cell wall, cell membrane, and middle lamella. Lignin is firmly combined with cellulose and hemicellulose. It fills the space between cellulose, hemicellulose, and pectin present in the cell wall, especially in the xylem tracheids, vascular structure, and sclereid cells. The primary role of lignin is to provide rigidity to strengthen the structure of cell walls, especially in stems and roots. It crosslinks polysaccharides to improve the mechanical strength of the cell walls and harden the whole plant.[14,15] It also blocks pathogen growth and protects plants by lignification of infections and wounds.[16]

In addition, lignin in the vasculature, a pathway for water transport, enables the vascular tissues of plants to transport water efficiently.[15] The polysaccharide component of the plant cell wall is hydrophilic and can enable water to permeate, whereas lignin is hydrophobic and impermeable to water. Therefore, hydrophobic lignin crosslinking with polysaccharides prevents moisture from passing through the cell wall.

2.1 Lignin extraction processes

Lignin is separated from lignocellulose and cellulose in the plant during chemical pulping processes. The different pulping processes result in various technical forms of lignin.[17] The four main types of technical lignin are classified according to sulfur or sulfur-free processes (Table 1). Sulfur processes include kraft processes and sulfite pulping. The kraft process breaks lignin down with a strong alkali solution, an aqueous solution of sodium hydroxide and sodium sulfide. Kraft-produced lignin is highly hydrophobic and has a high sulfur content at around 1 to 2 wt%.[18] Because of its relatively narrow dispersion, abundance, and low price, kraft lignin is commonly used in the development of lignin-based polymers.

The second process is sulfite pulping, which is the second most popular process. The sulfite process reacts wood or biomass with calcium or magnesium sulfite at 125–150 °C for 3–7 h, which then undergoes an acidic treatment instead of treatment with an alkali solution in kraft pulping. The product of sulfite pulping is lignosulfonate, which contains a considerable amount of sulfur (approximately 3.5–8 wt%) in the form of sulfonate groups on the aliphatic side chains. Due to the sulfonate polar group, lignosulfonate is soluble in water.[26,27]

Sulfur-free processes include soda processes and solvent pulping (organosolv). The soda process is the oldest pulping method and is mainly used to treat non-wood materials. The soda process is carried out under strongly basic conditions (pH = 11–13) with NaOH solution at a high temperature (150–170 °C). The difference from the kraft process is that it does not use a sulfur additive, so it is more similar to natural lignin than lignin from other processes. Therefore, it has more economical applications.

Organosolv lignin extraction employs organic solvents to extract lignin from biomass in the presence of acid or base catalysts. Ethanol, methanol, acetic acid, and formic acid are primarily used in this process and water is occasionally used alongside the organic solvent, serving as a solvent but not involved in extraction. During extraction, the α-aryl ether bonds predominantly break, while the β-aryl ether bonds are cleaved to a lesser extent. As a result of ether bond cleavage, new phenolic groups are formed, producing highly phenolic organosolv lignins. Despite their highly phenolic nature, organosolv lignins are relatively hydrophobic, have a low molecular weight, and are free of sulfur and impurities.[28–30] Organosolv lignin is hydrophobic, sulfur-free, and has a low molecular weight of around 5 kg mol^{-1}. On the other hand, it is recovered from the solvent by precipitation, which usually requires the adjustment of various parameters such as concentration, pH, and temperature. In this process, an organic solvent is used, which increases the process cost and decreases the economic efficiency.[31] Fig. 2 briefly describes each process and its major product.

Table 1 Annual production quantities and prices of various types of lignin

	Kraft lignin	Ligno sulfonate	Soda lignin	Organosolv lignin
Annual production (kton per year)	265 (ref. 158)	1315 (ref. 158)	75 (ref. 158)	113 (ref. 159)
Price ($ per Mton)	260–500 (ref. 160)	180–500 (ref. 160)	200–300 (ref. 161)	280–520 (ref. 160)

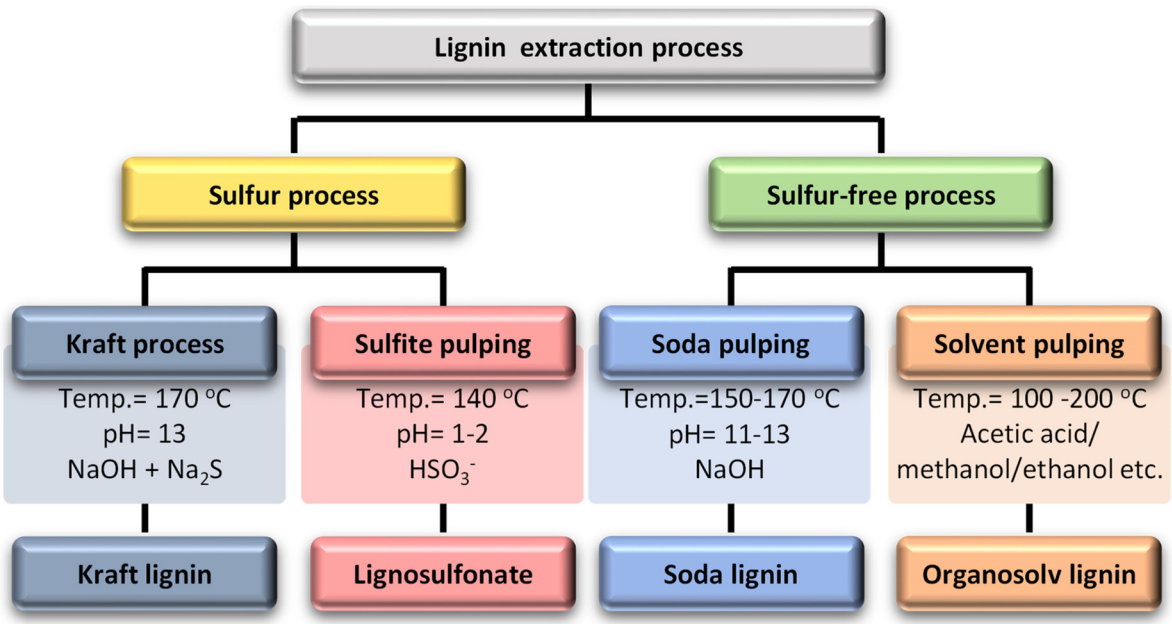

Fig. 2 Lignin extraction processes, process conditions, and their dominant products.[27]

2.2 Chemical structure of lignin

The chemical structure of lignin is a phenyl propane carbon skeleton with three carbons attached to the benzene ring. These have a three-dimensional network structure in which benzene rings and side chains are combined with each other (Fig. 3). The monomers that participate in the biosynthesis of lignin are collectively called monolignol, and there are three types: *p*-coumaryl alcohol, coniferyl alcohol, and sinapyl alcohol. Each monolignol is involved in the formation of *p*-hydroxyphenyl (H), guaiacyl, (G), syringyl (S), which are phenylpropanoid forms (Fig. 4a). The three types of monolignols are distributed in different combinations depending on the type of plant.

In biosynthesis, the phenylpropanoid monomers undergo an *in situ* radical coupling, making interunit linkages, such as aryl ether (α-O-4′ and β-O-4′), resinol (β-β′), phenyl coumaran (β-5′), biphenyl (5-5′), and 1,2-diaryl propane (β-1′) (Fig. 4b).[32] Among these interunit linkages, β-O-4′ is the most abundant linkage, almost 50% of the total interunit linkage in lignin. Also, the β-O-4′ linkage is the most important chemical linkage from the aspect of lignin depolymerization and fractionation. While the other linkages (β-5′, β-β′, 5-5′, β-1′) are more resistant to chemical degradation, β-O-4′ is one of the most commonly cleaved chemically, providing a basis for industrial processes such as chemical pulping.[16,33–35] Although ethers are usually relatively inert, they can be liable to cleavage because of the presence of lone-pair electrons on oxygen, which is a source of reactivity. The lone-pair electrons increase the polarity of the –C(β)–O– bond and make the neighboring β-carbon atom sensitive to nucleophilic attack. Additionally, the susceptibility of the β-O-4 linkage to undergo a cleavage reaction is dependent on whether the structure is phenolic or non-phenolic due to their reactivity differences.[34]

Although the chemical structure of lignin cannot be defined exactly in an easy way, it is already known that lignin has various functional groups, including methoxy, phenolic hydroxyl, aliphatic hydroxyl, and other carbonyl containing

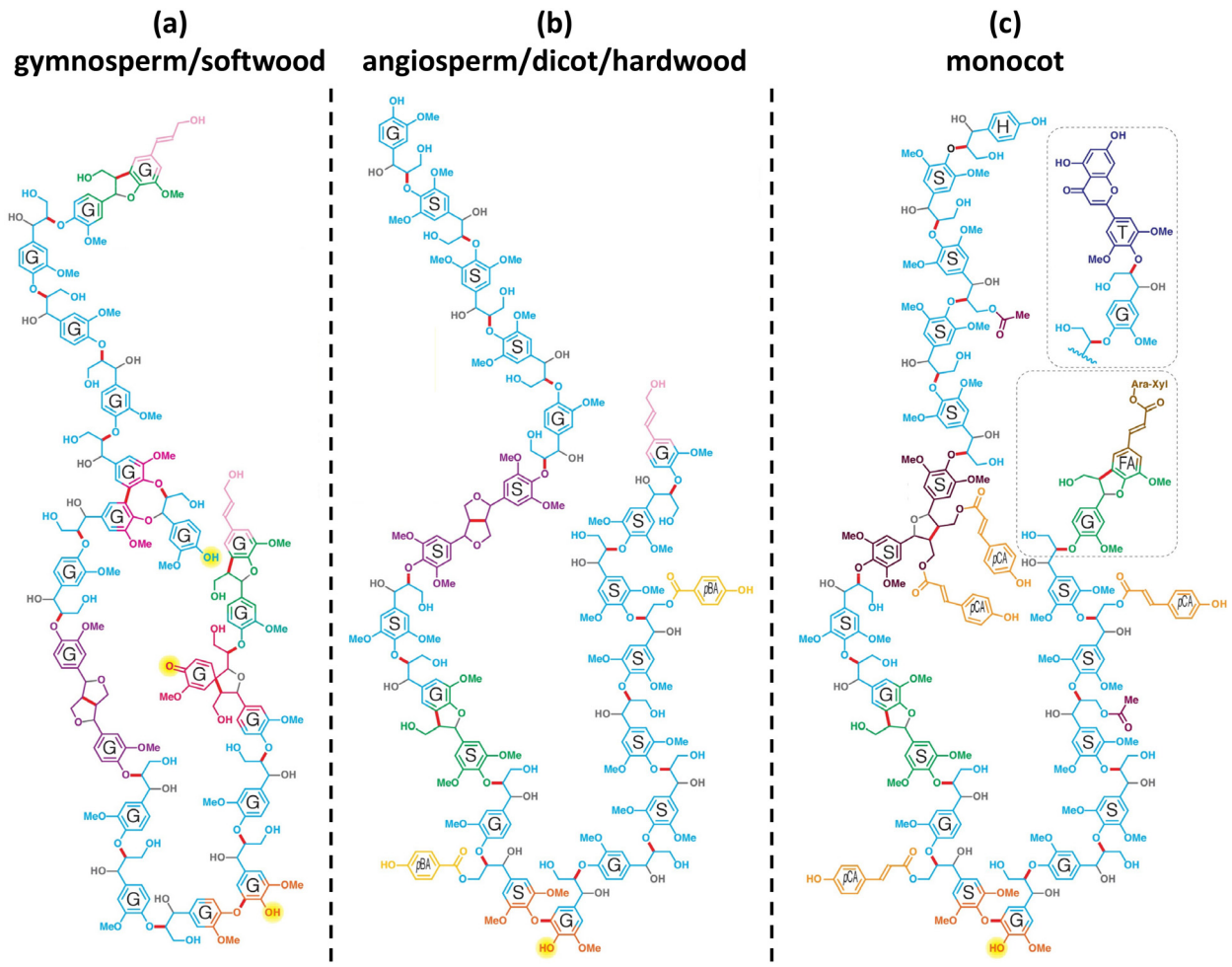

Fig. 3 Chemical structures of model lignin 20-mers: (a) gymnosperm/soft wood lignin, (b) angiosperm/dicot/hardwood lignin, and (c) monocot lignin. It is a model structure of lignin since the exact structure of lignin is not known. H: *p*-hydroxyphenyl unit, G: guaiacyl unit, S: syringyl unit, FA: ferulate, *p*CA: *p*-coumarate, *p*BA: *p*-hydroxylbenzoate, T: tricin, gray: oxygen or hydroxy groups that derive from water during quinone methide rearomatization, and the bonds to them. Reproduced from ref. 9 with permission from Elsevier Ltd., copyright 2019.

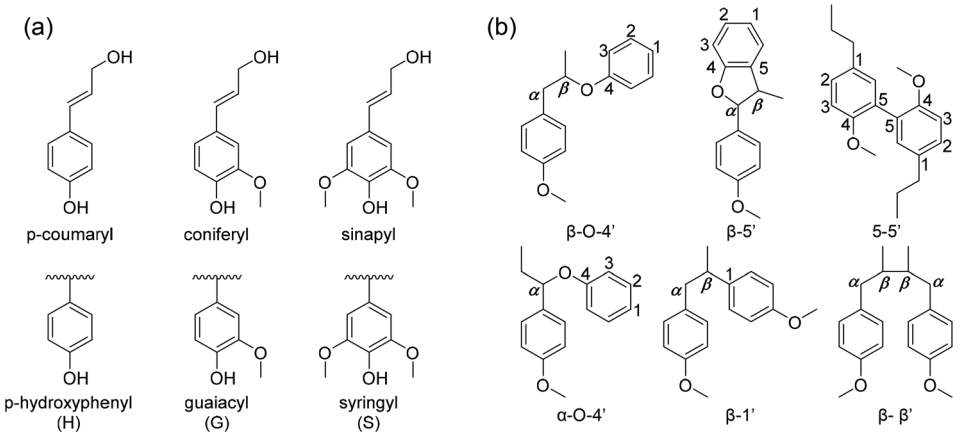

Fig. 4 (a) The precursors of lignin (H, G, S from *p*-coumaryl, coniferyl and synapyl respectively), (b) common linkages between phenyl propane units in lignin.

groups. Various commercial lignins and their hydroxyl group contents are summarized in Table 2. These functional groups provide reactive sites for the modification of lignin.

2.3 Modification of lignin

One of the most efficient modification methods of lignin is graft copolymerization. Graft copolymerization can functionalize lignin by integrating monomer or polymer chains to improve its properties. Especially, graft copolymerization can produce lignin-based polymers that possess precisely controllable architectures and specialized functional groups. A graft copolymer generally consists of a backbone polymer as the main chain and one or more branch polymers connected to the backbone *via* covalent bonds.[32] The properties of the copolymers produced are controlled by the functional groups on the grafted polymers, length of the graft, and graft density. There are three primary grafting methods: graft-from, graft-onto, and graft-through.

The "graft-from" method is a method in which a monomer reacts at an active site on a backbone polymer to grow a grafted polymer (Fig. 5a). In this method, lignin generally acts as a backbone polymer to provide hydroxyl groups as initiation

Table 2 Lignin sources and their hydroxyl group contents

Lignin description	Vendor	Hydroxyl group content (mmol g^{-1})	Reference
Kraft lignin	Jilin Paper Co., Ltd	Phenolic: 2.73	Lin *et al.*[19]
Kraft lignin, alkali	Sigma Aldrich	Phenolic: 3.0 Aliphatic: 4.41	Liu *et al.*[20]
Alkali lignin	Sigma Aldrich	11.24	Yu *et al.*[21]
Hardwood lignin	Sigma Aldrich	Phenolic: 3.2 Aliphatic: 2.9	Kim and Kadla[22]
Softwood lignin	TCI	4.48	Liu and Chung[23]
Softwood Kraft lignin	Mead Westvaco	Phenolic: 3.8 Aliphatic: 2.4	Argyropoulos *et al.*[24]
Organosolv lignin	Lignin Corporation	1.6	Korich *et al.*[25]

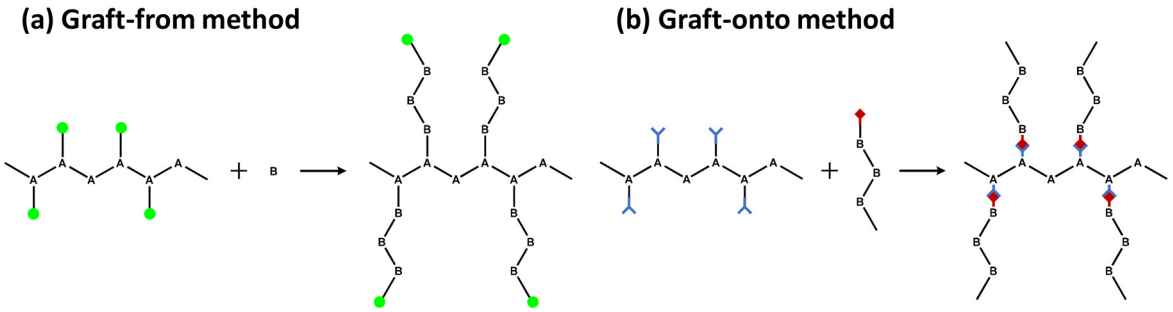

Fig. 5 (a) Graft-from and (b) graft-onto methods for the synthesis of graft copolymers.

sites. The other way is to modify the hydroxyl group of lignin to make a macroinitiator with functionalized initiation sites. The grafted polymer grows at the beginning of lignin by various polymerization methods, including ATRP (atom transfer radical polymerization), RAFT (reversible addition–fragmentation chain transfer polymerization), ring-opening polymerization, and free radical polymerization. As a result, the graft density of the copolymer synthesized by the graft-from method is generally higher than those from graft-onto method.

"Graft-onto" means that polymer chains, which are separately synthesized, covalently link to the surfaces of backbone polymer, lignin (Fig. 5b). The "graft-onto" method requires an efficient covalent bond formation reaction between the lignin backbone and the end groups of the graft polymer. "Graft-onto" can incorporate a variety of integrated reactions and polymers with convenient reaction conditions as well as a wider range of solvent selection and purification methods.[36] Click chemistry is the most commonly used synthesis method for grafting polymers onto lignin due to its high efficiency and ease of experimentation. Other reactivity including photoredox catalyzed thiol–ene reactions, base-catalyzed ring-opening reactions of epoxide, *in situ* free radical reactions, substitution, condensation, boronate ester formation, and crosslinking were successful methods for the preparation of lignin graft copolymers.[37]

In the "graft-through" method, ordinary monomers are polymerized in the presence of macromonomers so that the main chain is "sewn" through the ends of the side chains during the copolymerization process.[38] Due to the lack of a well-defined chemical structure and the irregular three-dimensional network structure of lignin, the number of studies on lignin-based copolymers prepared by this method are limited.

To summarize, lignin is a complex aromatic polymer with unique structural and chemical properties, making it a promising candidate for various applications, including as a feedstock for producing bio-based materials. Among these potential applications, graft copolymerization with aliphatic polyesters has garnered significant attention. Aliphatic polyesters, known for their biodegradability and flexibility, offer complementary properties that can be enhanced when combined with lignin. The copolymerization between lignin and aliphatic polyesters not only provides an opportunity to develop novel composite materials with improved mechanical and thermal properties but also contributes to the advancement of sustainable materials science. This transition from the aromatic, rigid nature of lignin to the aliphatic, flexible characteristics of polyesters sets the stage for exploring the potential benefits and challenges of their integration, which are discussed in the following section.

3. Aliphatic polyester

Because of environmental concerns and increased interest in biomedical applications, aliphatic polyesters have been put in the spotlight as an alternative biodegradable polymer material in recent decades. All polyesters are theoretically considered biodegradable because their main production reaction, esterification, is chemically reversible by hydrolase action and hydrolysis.[39] Although aliphatic polyesters are easy to biodegrade, they have low mechanical properties due to their linear chain structure compared to aromatic polyesters. Fig. 6 shows the chemical structures of a few representative biodegradable polymers (aliphatic polyesters). The polyester can be synthesized by a polycondensation reaction between (1) monomers containing a dihydroxyl group (diol) and monomers containing a dicarboxylic acid group,[40] (2) a diol and an anhydride,[41] (3) a diol and an acid chloride,[42] (4) a diol and a nitrile,[43] (5) a diol and carbon suboxide,[44] (6) a diol and an ester (transesterification),[45] and (7) a difunctional monomer with a hydroxyl group and a carboxylic acid,[46] and ring opening polymerization. The synthesized aliphatic polyesters showed good potential for applications in multiple fields including drug delivery systems,[47] packaging,[48] medical implants,[48] and films.[49]

3.1 Poly(lactic acid) (PLA)

One of the most studied aliphatic polyesters is poly(lactic acid) (PLA). PLA can be synthesized by polycondensation of lactic acid or ring opening polymerization of lactide. Lactic acid and lactide, which are monomers of PLA, are chiral molecules with two forms, L-form (L-lactic acid and L-lactide) and D-form (D-lactic acid and D-lactide). The tacticity of a polymer is determined by which isomers of monomers are bound. The homopolymers of the L-form (PLLA) and D-form (PDLA) are isotactic polymers and the copolymer of the L-form and D-form (PDLLA) is an atactic polymer (Scheme 1). The crystallinity, mechanical

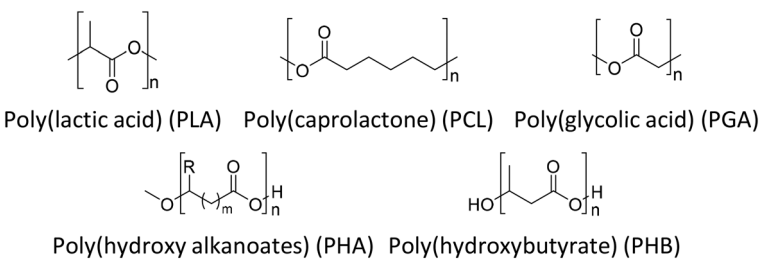

Fig. 6 Chemical structures of a few representative biodegradable polymers, aliphatic polyesters.

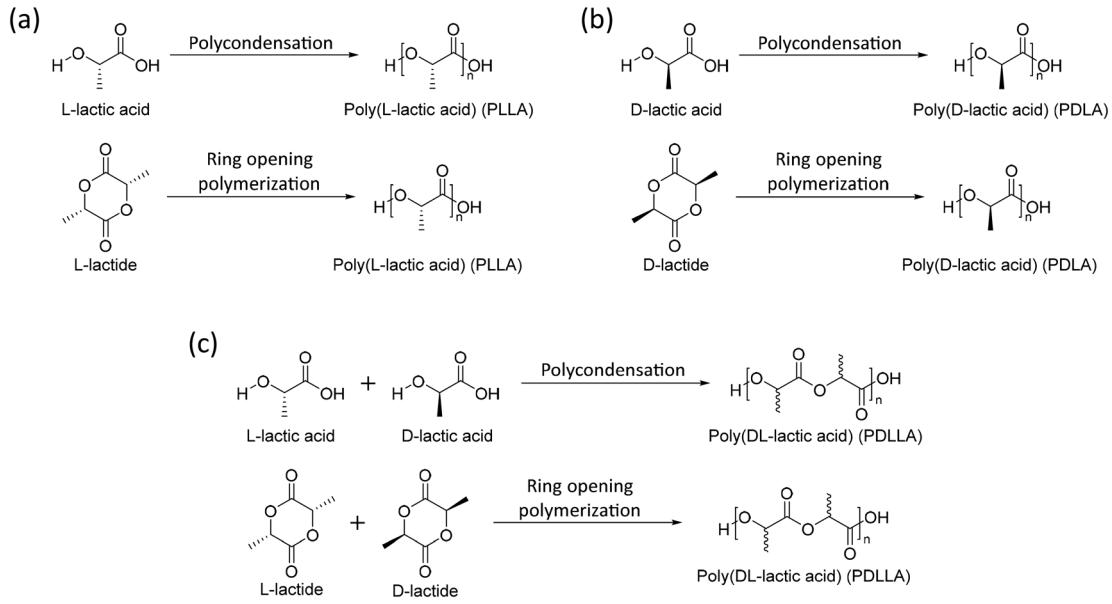

Scheme 1 Synthesis of (a) poly(L-lactic acid) (PLLA), (b) poly(D-lactic acid) (PDLA), (c) poly(DL-lactic acid) (PDLLA).

properties, and biodegradability rate of polymers determine the tacticity. Isotactic polymers (PLLA and PDLA) are semi-crystalline polymers with relatively high mechanical strength and low degradation rates, whereas an atactic polymer (PDLLA) results in amorphous and low mechanical properties and high degradation rates. Because of these properties, PLLA and PDLA were used in orthopedic and fixation devices.[42] On the other hand, PDLLA is used in biomedicine for tissue engineering[50] and drug delivery devices.[51]

3.2 Poly(glycolic acid) (PGA)

Poly(glycolic acid) (PGA) is another aliphatic polyester that can be synthesized by polycondensation and ring opening polymerization (Scheme 2a). Glycolic acid and glycolide, monomers of PGA, are simpler than lactic acid and lactide and have no chirality, thus its polymer, PGA, has no tacticity. It results in high crystallinity (45–55%) with a high melting temperature (T_m, 220–225 °C).[52] Also, PGA has a faster degradation rate and better mechanical properties than PLA.[53] Based on these properties, glycolic acid is used to synthesize a copolymer, poly(lactic acid-*co*-glycolic acid) (PLGA), with lactic acid by polycondensation (Scheme 2b). The properties of PLGA are controlled by the molar ratio between lactic acid and glycolic acid. Due to its biodegradable nature, excellent biocompatibility, low toxicity, high miscibility with other polymers, and the ability to form films and capsules, PLGA finds extensive use in drug delivery systems.[54]

3.3 Poly(caprolactone) (PCL)

Recently, aliphatic polyesters obtained from macro lactones have been investigated for their more favorable ductility and strength properties over poly(lactic acid), which are intrinsically brittle.[55,56] One of them is poly(caprolactone) (PCL). It is not only an FDA approved material but also a traditional material for applications in biomedicine[57] and food packaging.[58] PCL was first synthesized by the Carothers group in the early 1930s.[59] PCL is mainly synthesized by ring-opening polymerization of ε-caprolactone (Scheme 3). The homopolymer of PCL requires up to four years for complete degradation.[60] Because of the biodegradability and biocompatibility

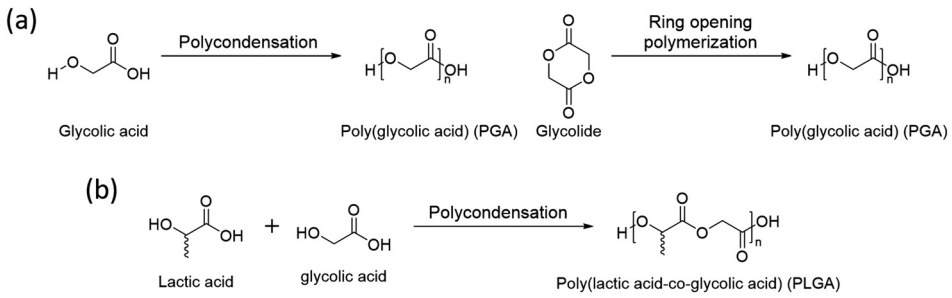

Scheme 2 Synthesis of (a) poly(glycolic acid)(PGA) and (b) poly(lactic acid-*co*-glycolic acid) (PLGA).

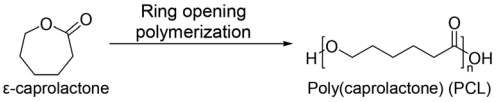

Scheme 3 Synthesis of poly(caprolactone) (PCL).

of PCL, PCL is employed in various applications, including drug delivery, dentistry, tissue engineering, and several medical devices. Many drug delivery devices made from PCL have been approved by the FDA. Also, diverse medical devices are assembled with PCL copolymers. PCL has good solubility in organic solvents and a low T_m of 60 °C.[59] These features enable convenient copolymerization with other synthetic polymers. For example, poly(caprolactone)-*block*-poly(glycolic acid) is commercialized as a monofilament suture,[61] and tissue-reinforcing patches composed of poly(caprolactone)-based polyurethane have been developed.[62]

3.4 Poly(ethylene brassylate) (PEB)

An example of an aliphatic polyester obtained from a macro lactone is PEB, a relatively unexplored polymer compared to PCL. Research on PEB began in 2014, and as of August 2024, fewer than 100 references to it are found on Web of Science. The most common method used to obtain PEB is the ring-opening polymerization of ethylene brassylate. The first method reported by Kobayashi *et al.* in 1999 used lipase enzymes as a catalyst.[63] However, this method yielded low molecular weight polymers. In 2014, Pascual *et al.* reported organic base-catalyzed PEB polymerization.[64] The superbase 1,5,7-triazabicyclo[4.4.0]dec-5-ene (TBD) showed the highest polymerization efficiency, the fastest reaction rate, the highest molecular weight, and the narrowest PDI value among all compared conditions. The same research group showed pioneering works in their study of PEB, including utilizing TBD as both the initiator and catalyst of the ring opening polymerization of ethylene brassylate (Scheme 4).[64–66]

PEB has high potential for being a commercially useful, sustainable raw material for polymers. This is because the monomer, ethylene brassylate, is derived from non-human food vegetable oil (castor oil), which is cheap and highly abundant. Ethylene brassylate is a commercially available 17-membered ring lactone and is much cheaper than lactide and other macro lactones, such as ε-caprolactone. A large production infrastructure of ethylene brassylate has already been established in the fragrance industry.[67] Briefly, ethylene brassylate can be easily obtained from tridecanoic acid synthesized from 10-undecanoic acid,[68] which is an unsaturated fatty acid extracted from castor plants.

The thermal properties of PEB are similar to those of polycaprolactone, but PEB exhibits a slightly higher T_m of 68.1 °C (M_n = 18 kDa, DP = 66) to 73.3 °C (M_n = 137 kDa, DP = 508)[83] compared to PCL, which has a T_m of 56.0 °C (M_n = 10 kDa, DP = 87) to 62.7 °C (M_n = 80 kDa, DP = 701).[84] The glass transition temperature (T_g) follows the same trend, with a T_g of −30 °C for PEB and a T_g of −60 °C for polycaprolactone.[85–87] The renewable and biobased natures of PEB are desirable features (Table 3). However, its mechanical properties need to be improved for advanced applications. Enhanced mechanical properties, such as the tensile strength and modulus, will enable it to replace commercial polyolefins.

3.5 Poly(hydroxy alkanoate) (PHA)

PHAs are a family of biological polyesters that contain hydroxy alkanoate monomer units.[88,89] PHA can usually be obtained from bacteria and archaea[90] and synthesized with a polymerizing enzyme. During biosynthesis, all monomer units are in the *R* configuration due to the enzyme's stereospecificity, which provides the optical activity of the synthesized polymer.[89] Examples of PHA families are poly(4-hydroxybutyrate) (P4HB), poly(3-hydroxybutyrate) (P3HB), poly(3-hydroxyoctanoate) (PHO), poly (3-hydroxybutyrate-*co*-3-hydroxyvalerate) (PHBV), and poly(3-hydroxybutyrate-*co*-3-hydroxyoctanoate) (PHBHHx).[90]

The biosynthetic pathways for the majority of PHA monomers are derived from various carbon sources such as glucose and fatty acids, which are primarily related to essential carbon metabolic pathways, including glycolysis, β-oxidation, and the synthesis of new fatty acids (Fig. 7). Moreover, structurally similar carbon sources such as γ-butyrolactone (GBL)/4HB of 1,4-butanediol (BDO), 3-hydroxyvalerate (3HV) of propionate, and 3-hydroxypropionate (3HP) of 1,3-propiondiol (PDO) can serve as precursors. Additionally, medium and long-chain lengths of other fatty acids, like 3-hydroxyalkanoate (3HA), have a significant impact on the material's properties (Table 4).[89,91,92] Consequently, by supplying tailored feedstocks (Fig. 7), various PHA homopolymers and copolymers can be obtained with engineered microorganisms.[93]

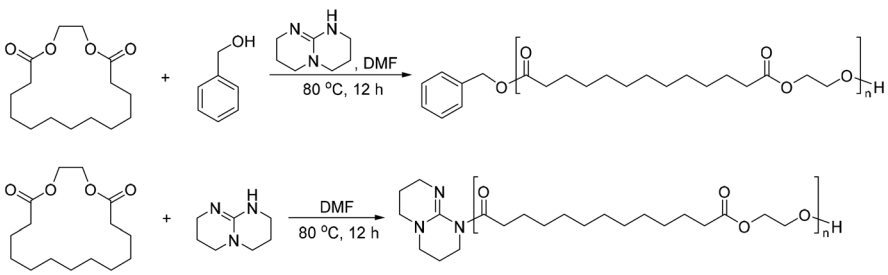

Scheme 4 Synthesis of poly(ethylene brassylate) (PEB) *via* ring-opening polymerization.

Table 3 Synthesis of PHA from various microorganisms

No.	Polymer	Microbial strain	Source	Reference
1	PHA	Recombinant *E. coli*	Cheese whey	Pais *et al.* (2014)[69]
2		*Halomonas hydrothermalis*	Seaweed-derived crude levulinic acid, containing formic acid, residual sugars, and dissolved minerals	Bera *et al.* (2015)[70]
3		*T. thermophilus* HB8	Lactose from whey-based media	Pantazaki *et al.* (2009)[71]
4	P3HB	Recombinant *E. coli* BL21	Glucose	Lin *et al.* (2017)[72]
5		*Cupriavidus necator* DSM 545	Glucose, acetic acid	Marudkla *et al.* (2018)[73]
6		*Ralstonia eutropha*	Sucrose	Park *et al.* (2015)[74]
7		*Cupriavidus necator* NSDG-GG	Glucose, urea	Biglari *et al.* (2018)[75]
8		Marine *Bacillus megaterium* UMTKB-1 strain	Glycerol	Yatim *et al.* (2017)[76]
9		Endophytic *Bacillus cereus* RCL 02	Valeric acid	Das *et al.* (2018)[77]
10		*Paracoccus denitrificans* DSMZ 413	Glycerol	Kalaiyezhini *et al.* (2015)[78]
11		*Acinetobacter junii* BP 25	Parboiled rice mill effluent	Sabapathy *et al.* (2018)[79]
12	P4HB	Recombinant *Escherichia coli*, like JM109	Propionic acid, glycerol	Malacara *et al.* (2015)[80]
13	PHO	Recombinant *Cupriavidus necator* strains	Canola oil	Valdés *et al.* (2018)[81]
14		*Pseudomonas putida* and *Bacillus subtilis*, at a rate of 3 : 1	Sodium octanoate	Eremia *et al.* (2016)[82]

3.6 Degradation of aliphatic polyester *via* hydrolysis

The degradation of polyesters occurs through hydrolysis in the presence of acid or base catalysts.[94] Under acidic conditions, the degradation of polyesters begins with protonation of the carbonyl oxygen of the ester group by a hydronium ion, which makes the carbonyl carbon more electrophilic due to the positive charge. The next step is that water molecules attack the carbonyl carbon, which generates a tetrahedral intermediate. The tetrahedral intermediate can decompose into a carboxylic acid and a hydroxyl group, or back the polyester structure (Scheme 5).[94]

Under basic conditions, degradation begins with attack of the hydroxide anion on the carbonyl carbon of the ester group, generating a tetrahedral intermediate. The tetrahedral intermediate can decompose into a carboxylic acid and a hydroxyl group. The preference of the tetrahedral intermediate toward hydrolysis or ester regeneration is determined by the leaving ability of the hydroxyl group and stabilizing a negative charge (Scheme 6).[94,95] The enzyme-mediated biodegradation of aliphatic polyesters is described elsewhere with detailed information.[96–100]

4. Lignin-*graft*-polyester

In this section, we discuss lignin-based copolymers that have covalent linkages between lignin and its counterpart polymers. Especially, we focus on lignin-*graft*-polyester, not derivatives or depolymerized lignin-based polymer. Lignin-*graft*-polyester exhibits several characteristics that make it particularly suitable for green chemistry.

Firstly, as discussed in section 2, lignin is a natural polymer extracted from wood and other plants, constituting a significant component of biomass. Utilizing lignin leverages renewable resources, reduces reliance on fossil fuel-based materials, and contributes to a lower environmental impact.

Secondly, the direct use of lignin for polymer synthesis circumvents the environmentally harmful depolymerization processes of lignin, thereby conserving energy and minimizing pollutant emissions. Depolymerizing lignin into smaller molecules often requires substantial energy and can produce various environmental pollutants. For instance, the chemical or thermal treatments used to break down lignin into monomers and other fine chemicals involve significant amounts of organic solvents and energy, which can have detrimental environmental effects. The organic solvents typically used in lignin depolymerization do not align with the principles of green chemistry. These solvents are often toxic or highly volatile, posing risks to both the environment and human health. Therefore, the lignin-*graft*-polyester research discussed supports the principles of a circular economy, decreasing the environmental burden associated with waste management.

Thirdly, lignin-*graft*-polyester can retain the functional properties of polymers and the biodegradability of natural materials. This ensures that end-of-life lignin-*graft*-polyesters can decompose naturally in the environment, minimizing their ecological footprint compared to non-degradable conventional petroleum-based polymers. In addition, recent studies have proved that lignin-*graft*-polyesters are excellent materials that address the shortcomings of previously developed aliphatic polyesters and provide additional functions based on the high aromaticity of lignin.

In summary, lignin-*graft*-polyesters are well-suited for green chemistry due to the renewable nature of lignin, the avoidance of energy-intensive and polluting depolymerization processes, the minimization of harmful organic solvents, waste reduction, and inherent functionality and biodegradability of the resulting materials. These advantages position lignin–polyester copolymers as promising candidates for sustainable materials.

The representative grafted polymers on lignin are PLA and PCL. The lignin-*graft*-polyesters provide cost-efficiency, high mechanical properties, adhesion properties, flame retardancy, antioxidant properties, and antimicrobial properties.[101]

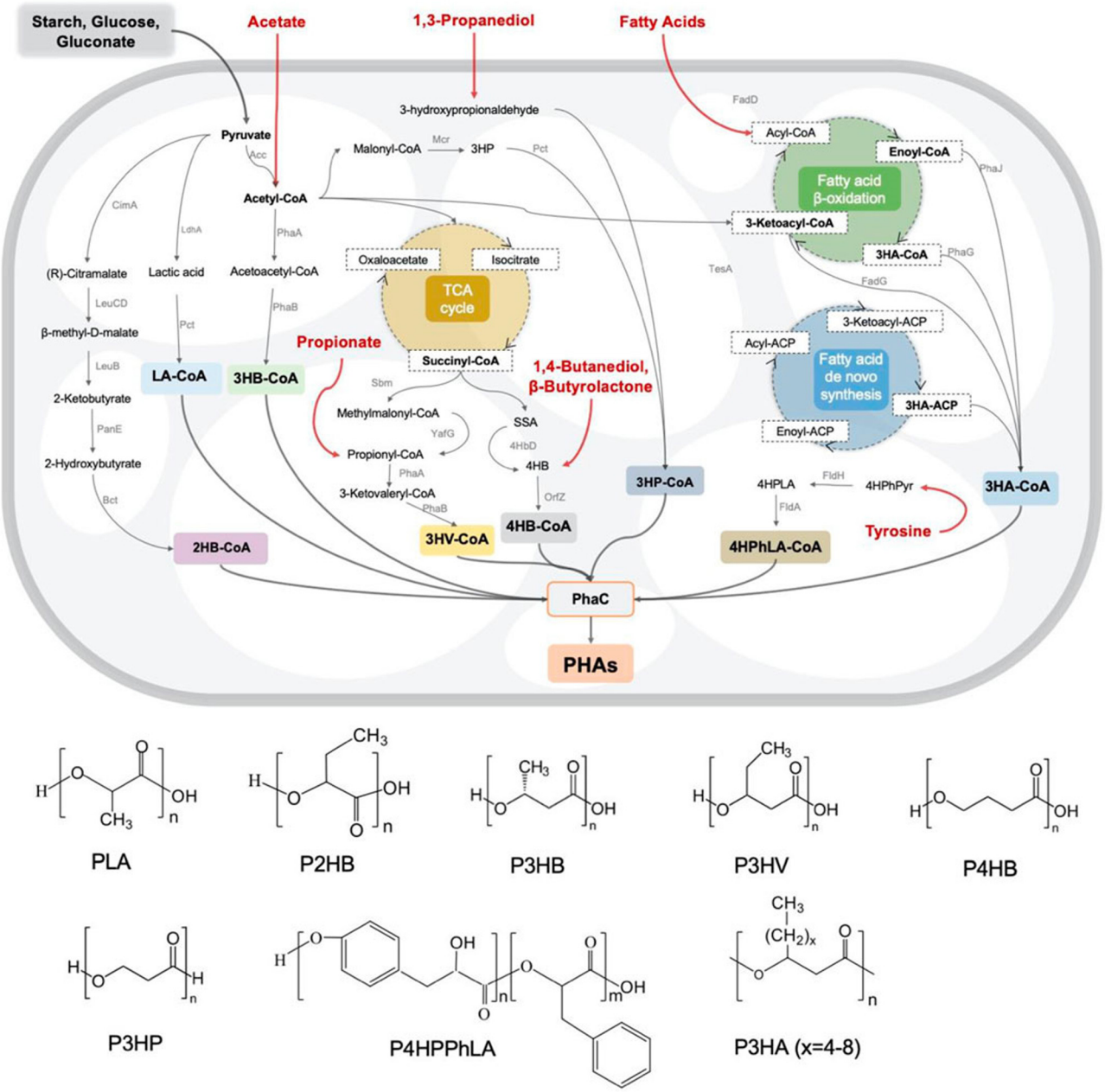

Fig. 7 Metabolic pathways and monomer structures of different microbially synthesized PHAs. Reproduced from ref. 93 with permission from Frontiers Media S.A., copyright 2022.

Table 4 Physical properties of polyesters

Polymer	Melting point (°C)	Glass transition temperature (°C)	Crystallinity	Mechanical strength
Poly(lactic acid) (PLA)	170–180 (ref. 84)	60–65 (ref. 84)	Semi-crystalline (PLLA and PDLA), amorphous (PDLLA)	High strength in isotactic forms (PLLA/PDLA), low in atactic (PDLLA)
Poly(glycolic acid) (PGA)	220–225 (ref. 52)	35–40 (ref. 52)	High (45–55%)	Higher mechanical strength and faster degradation compared to PLA
Poly(caprolactone) (PCL)	56–63 (ref. 84)	−60 (ref. 84)	Semi-crystalline	Good ductility and strength
Poly(ethylene brassylate) (PEB)	68–73 (ref. 83)	−30 (ref. 83)	Semi-crystalline	Needs to be improved for advanced applications
Poly(hydroxy alkanoate) (PHA)	Variable	Variable	Variable	Variable

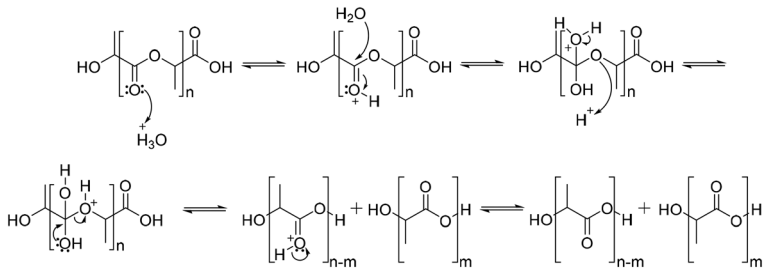

Scheme 5 Hydrolysis mechanism of poly(lactic acid) under acidic conditions.

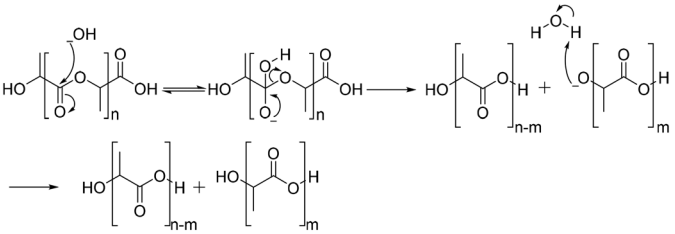

Scheme 6 Hydrolysis mechanism of poly(lactic acid) under basic conditions.

4.1 Lignin-*graft*-poly(lactic acid) (lignin-*graft*-PLA)

Lignin-*graft*-PLA can be synthesized by both "graft-from" and "graft-onto" methods. The graft-from methods for the synthesis of a lignin-*graft*-PLA copolymer are reported in the literature several times.[102–105]

In 2013, Chung *et al.* reported the synthesis of lignin-*graft*-PLA through ring-opening polymerization in the presence of a TBD catalyst by initiating the hydroxyl group of lignin. The authors found that the grafting efficiency in lignin-*graft*-PLA synthesis from aliphatic hydroxyl groups was higher than for phenolic hydroxyl groups (Scheme 7a).[102] Also, Liu *et al.* and

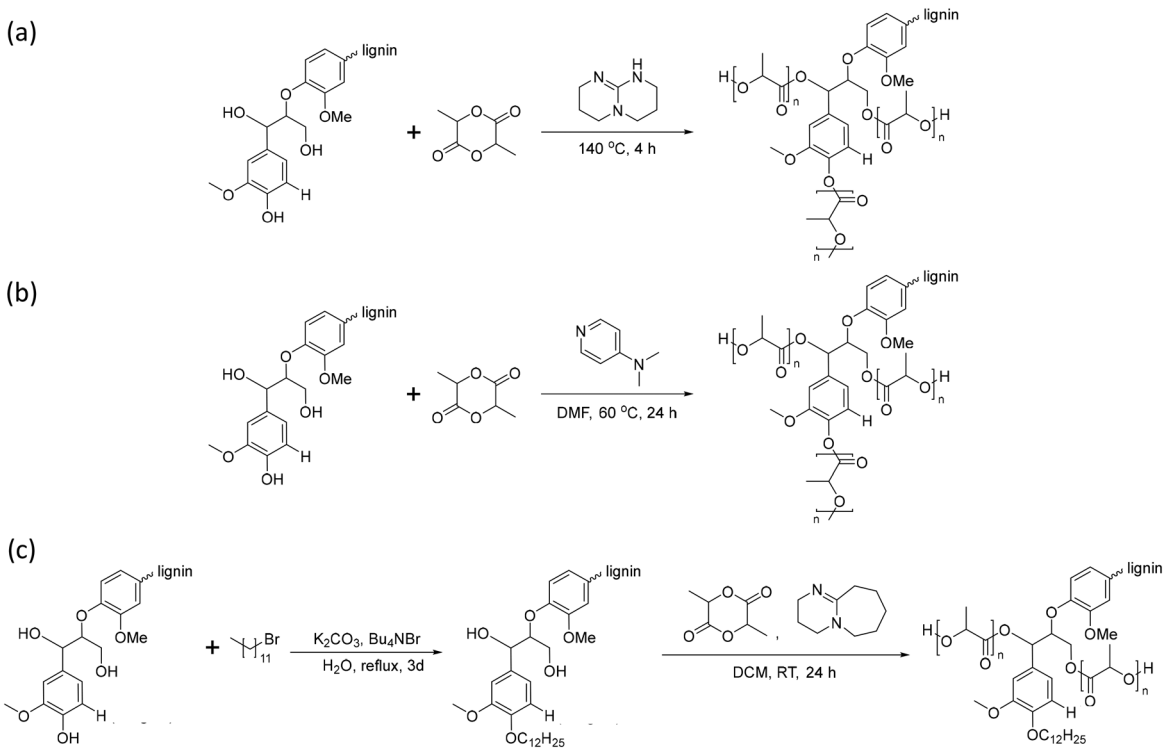

Scheme 7 (a) Synthesis of lignin-*graft*-PLA with TBD as a catalyst through a graft-from method. (b) Synthesis of lignin-*graft*-PLA with DMAP as a catalyst through a graft-from method. (c) Synthesis of dodecylated lignin-*graft*-PLA. Terminal β-O-4 softwood lignin unit is used for simplicity.

Dai *et al.* introduced a synthesis method using 4-dimethyl pyridine (DMAP) as a catalyst (Scheme 7b).[103,104]

In 2016, Ren *et al.* presented dodecylated lignin-*graft*-PLA to grow the high molecular weight of PLA (Scheme 7c).[105] Acetylation and butylation of lignin have been applied to reduce the number of hydroxyl groups. Reactions usually occur at the aliphatic hydroxyl groups, which are the preferred position for growing PLA. The authors reported a method for selective dodecylation to the phenolic hydroxyl group without interfering with the growth of PLA.

Lignin-*graft*-PLA synthesized by a graft-onto method was reported by Chile *et al.* in 2018.[106] PLA was separately synthesized by ring opening polymerization in the presence of $[(NNO)InCl]_2$ (μ-Cl)(μ-OEt), and the end group of PLA was modified as the chloride derivative. The modified PLA-Cl was grafted onto lignin with K_2CO_3 in DMF. When comparing the ratio of lignin to PLA in the produced polymer, the graft-onto method showed a higher lignin portion than the graft-from method for lignin-*graft*-PLA (Scheme 8).

Recently, grafting methods, including graft-from and graft-onto, *via* reactive extrusion were reported.[107–109] Reactive extrusion is a process that combines chemical reactions with extrusion, typically used in polymer processing. In this technique, the chemical reaction occurs within the extruder, allowing for the continuous formation and shaping of polymers or composites. This process is particularly useful for polymer modifications such as crosslinking, grafting, or blending, as it offers advantages like controlled reaction conditions, efficient mixing, and reduced processing time. The key benefits of reactive extrusion include the ability to conduct reactions under high shear and temperature, precise control over the reaction environment, and the potential for industrial-scale production.

In 2023, Makri *et al.* synthesized lignin-*graft*-PLA through reactive extrusion, employing both graft-from and graft-onto methods.[108] For the graft-from approach, the appropriate amount of lignin was premixed with L-lactide and a catalyst system consisting of triphenyl phosphine (TPP) and Sn $(Oct)_2$. This mixture was then fed into a rheometer (Brabender® Plasti-Corder® Lab-Station torque rheometer) set at 180 °C with a screw speed of 50 rpm, under a nitrogen atmosphere. The reaction was carried out for approximately 20 min. For the graft-onto method, PLA and lignin were premixed and fed into the same rheometer using a pneumatic ram, mixed at 180 °C with a screw speed of 50 rpm for 5 min. In this step, the catalyst is not required to form a graft copolymer.

The main application of lignin-*graft*-PLA is as an additive for a commercial polymer matrix to improve its optical and mechanical properties.[102,105,106,110] In 2013, Chung *et al.* reported on a PLA/lignin-*graft*-PLA composite.[102] The synthesized lignin-*graft*-PLA showed good dispersity, whereas unmodified lignin formed phase separated particles in the PLA matrix (Fig. 8a–e).

The PLA/lignin-*graft*-PLA composite with 1% lignin blocked the entire UV-C (100–280 nm) and UV-B (280–315 nm) regions, and it blocked 40–85% of UV-A (315–400 nm) depending on

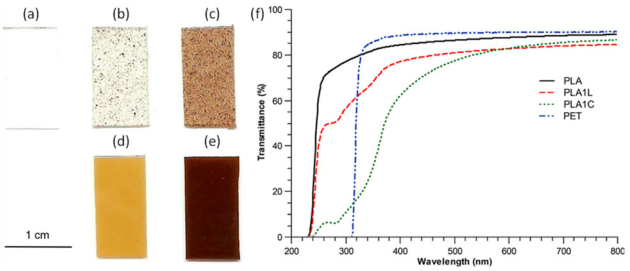

Fig. 8 Images of PLA–lignin composite samples suggest increased dispersion of lignin in composites made from lignin-*g*-PLA copolymer compared to those made with unmodified lignin: (a) PLA, (b) PLA with 1 wt% of lignin, (c) PLA with 5 wt% of lignin, (d) PLA with 1 wt% of lignin and 10 wt% of lignin-*g*-PLA copolymers, (e) PLA with 5 wt% of lignin and 12.5 wt% of lignin-*g*-PLA copolymer. (f) UV–vis spectra of PLA, PET, and PLA–lignin composites with unmodified lignin (PLA1L) and lignin-*g*-PLA copolymers (PLA1C). The amounts of lignin in the PLA films with unmodified lignin (PLA1L) and with lignin-*g*-PLA copolymers (PLA1C) are 1% and 0.9%, respectively. Reproduced from ref. 102 with permission from American Chemical Society, copyright 2013.

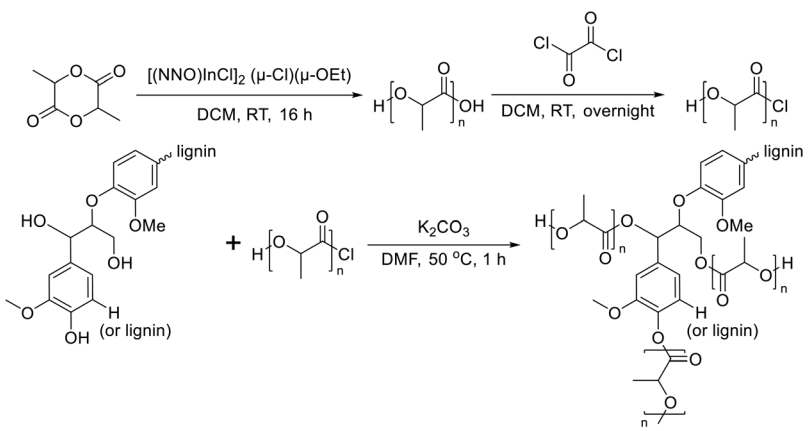

Scheme 8 Synthesis of PLA and graft copolymerization of PLA onto lignin. Terminal β-O-4 softwood lignin unit is used for simplicity.

the wavelength. However, the PLA matrix without the lignin component blocked only 25% of UV light above 250 nm (Fig. 8f). Also, PLA/lignin-*graft*-PLA composite with 1% lignin showed an increase in the tensile strength (+16%) and strain (+9%) compared to PLA (Fig. 9).

Zong *et al.* introduced PLA foam with lignin-*graft*-PLA in 2020.[111] First, they blended PLA and lignin-*graft*-PLA to make PLA/lignin-*graft*-PLA composite sheets. The sheets were placed in a high-pressure vessel and 15 MPa of CO_2 was applied to manufacture PLA/lignin-*graft*-PLA composite foam. The rheological, mechanical, and thermal properties of the prepared foam are investigated. The storage modulus of the PLA/lignin-*graft*-PLA samples decrease as the lignin-*graft*-PLA content increases. This behavior is attributed to the plasticization effect of lignin-*graft*-PLA on PLA. It increases the polymer chain spacing (free volume) of PLA and reduces entanglement between molecular chains (Fig. 10a).

The T_g and cold crystallization temperature of the PLA/lignin-*graft*-PLA samples decrease with the addition of lignin-*graft*-PLA. In addition, the crystallinity was increased to 7.1–12.4% compared to neat PLA. This is due to the good compatibility between lignin-*graft*-PLA and the PLA matrix, which prevents the uneven distribution of lignin-*graft*-PLA and ensures superior nucleation of lignin-*graft*-PLA. As a result, the diffusion of chain segments and the speed of chain arrangement improved the crystallization rate of PLA/lignin-*g*-PLA (Fig. 10b).

The size distribution of pores in foam samples was confirmed by SEM images of PLA/lignin-*graft*-PLA foams (Fig. 11a–e). The composite form of PLA with 3% of lignin-*graft*-PLA showed a smaller average cavity cell size (30.6% smaller), higher cell density (two orders of magnitude higher), and a higher expansion ratio (about 150% higher) than pure PLA foams. This is attributed to the formation of a relatively smaller size and larger number of spherocrystals of PLA, resulting from the heterogeneous nucleation of lignin-*graft*-PLA.

Liu *et al.* investigated the influence of PLA tacticity on the thermal and mechanical properties (Fig. 12).[112] Lignin-*graft*-PDLA, lignin-*graft*-PLLA, and lignin-PDLLA were prepared by ring opening polymerization of L-lactide, D-lactide, and L-lactide/D-lactide mixture, respectively and these were used for making a blend film with PLLA. The

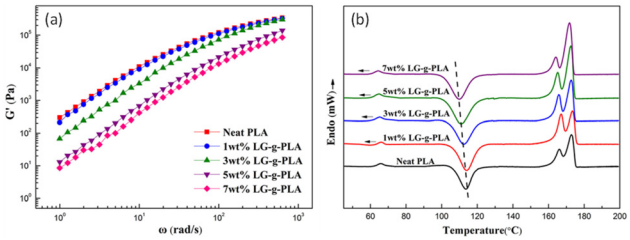

Fig. 10 (a) Storage modulus of PLA with different LG-*g*-PLA contents and (b) DSC curves of the PLA/LG-*g*-PLA and PLA samples. Reproduced from ref. 111 with permission from John Wiley and Sons, copyright 2020.

crystallization behavior and thermal stability of lignin-*graft*-PLAs were investigated. PLLA/lignin-*graft*-PDLA showed the fastest crystallization half-time, the highest crystallinity, and the highest T_g. Also, PLLA/lignin-*graft*-PDLA was the most stable at high temperature. On the other hand, PLLA/lignin-*graft*-PLLA showed the slowest crystallization half-time, the lowest crystallinity, the lowest T_g, and the lowest thermal stability (Fig. 13). The reason is that PDLA and PLLA form a triclinic racemic structure, known as a stereocomplex. Within the stereocomplex, left- and right-handed molecules pack side by side *via* van der Waals interactions, increasing the likelihood of forming zip-lock hooks. This zip-lock hook structure influences the crystallization behavior of PLLA.[113]

4.2 Lignin-*graft*-poly(caprolactone) (lignin-*graft*-PCL)

For lignin-*graft*-PCL, the most common synthesis method is graft-from copolymerization.[114–119] In 2013, Laurichesse *et al.* reported the synthesis of lignin-*graft*-PCL by ring opening polymerization in the presence of stannous octanoate ($SnOct_2$) catalyst and hydroxyl initiation sites on lignin.[117] The crystallinity of lignin-*graft*-PCL increased with a higher molar ratio of caprolactone. Lauricheese *et al.* employed dry toluene solvent, while Wang *et al.* and Park *et al.* utilized graft-from methods for lignin-*graft*-PCL, which was synthesized under solvent-free conditions using the same catalyst, $SnOct_2$ (Scheme 9).[118,119] Another catalyst, $ZnCl_2$, was used by Abdollahi *et al.* to prepare lignin-*graft*-PCL.[116]

The polymerization of ε-CL with $Sn(Oct)_2$/lignin is proposed to occur through a coordination mechanism, as depicted in

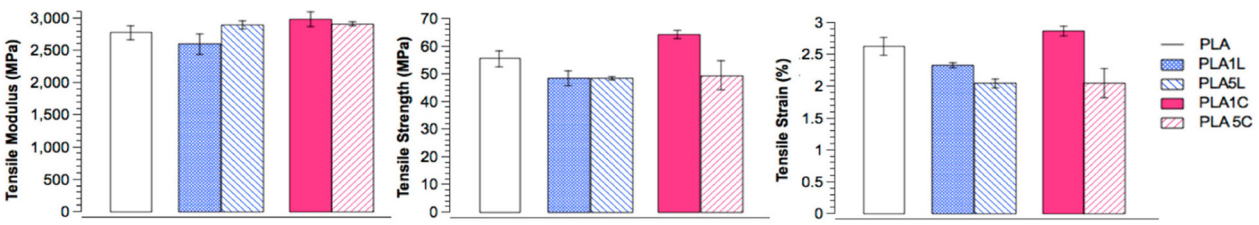

Fig. 9 Mechanical properties of PLA–lignin composites. The lignin contents in PLA1L/PLA1C and PLA5L/PLA5C are 0.9–1.0 and 4.4–4.8 wt%, respectively. Reproduced from ref. 102 with permission from American Chemical Society, copyright 2013.

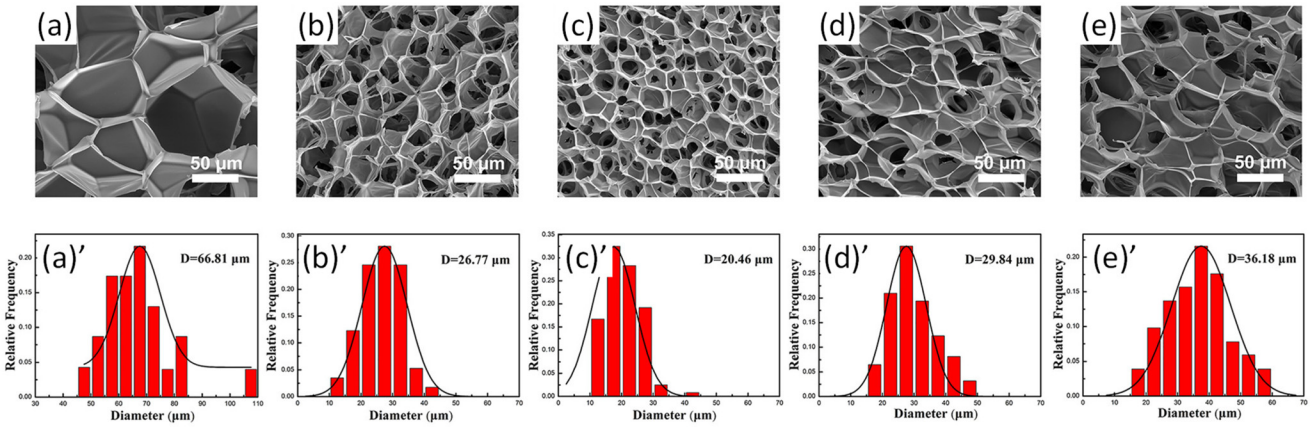

Fig. 11 (a)–(e) SEM images of cell morphology; (a)′–(e)′ corresponding cell size distributions of the PLA and PLA/lignin-*graft*-PLA foams: (a) and (a)′ neat PLA, (b) and (b)′ 1 wt% lignin-*graft*-PLA, (c) and (c)′ 3 wt% lignin-*graft*-PLA, (d) and (d)′ 5 wt% lignin-*graft*-PLA, and (e) and (e)′ 7 wt% lignin-*graft*-PLA. Reproduced from ref. 111 with permission from John Wiley and Sons, copyright 2020.

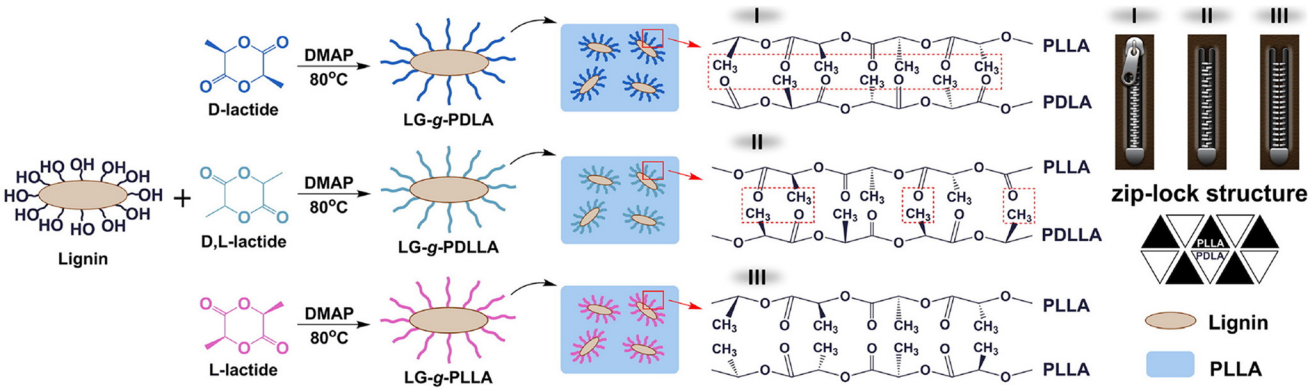

Fig. 12 Illustration of the synthesis of LG-*g*-PDLA (-PDLLA, -PLLA) and structures of the stereocomplex films. Reproduced from ref. 112 with permission from Elsevier, copyright 2017.

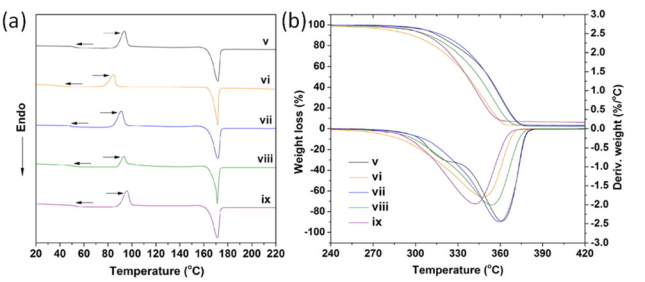

Fig. 13 (a) DSC heating curves related to the second heating scan, (b) TGA and DTG curves of PLLA and PLLA complex films. v: PLLA, vi: PLLA/3% lignin, vii: PLLA/3% lignin-*g*-PDLA, viii: PLLA/3% lignin-*g*-PDLLA, ix: PLLA/3% lignin-*g*-PLLA. Reproduced from ref. 112 with permission from Elsevier, copyright 2017.

Scheme 10.[120–124] Initially, Sn(II) alkoxide is generated through exchange reactions between $Sn(Oct)_2$ and the hydroxyl group of lignin. Once the authentic initiator is formed, initiation commences with the coordination of the carbonyl oxygen of ε-CL with tin. Subsequently, the nucleophilic oxygen in Sn–O-lignin attacks the carbonyl carbon of ε-CL, leading to cleavage of the acyl–oxygen bond in the ε-CL ring. This process results in the creation of the propagating species (–SnO–), and the propagation step advances by inserting ε-CL into the reactive Sn–O bond found in these active species.

In 2012, Korich *et al.* reported a graft-onto method to prepare lignin-*graft*-PCL.[25] In the first step, Bpin-PCL-OH was synthesized by ring opening polymerization using a pinacol boronate ester (Bpin)-containing initiator. Then, the hydroxyl end group of Bpin-PCL-OH was functionalized as an acylate end group and Bpin was deprotected as $B(OH)_2$ on ion exchange resin. As-prepared $B(OH)_2$-PCL-OAc was reacted with the hydroxyl groups of lignin to form aryl boronate ester bonds (Scheme 11).

Another graft-onto method for lignin-*graft*-PCL, using click chemistry, was studied by Han *et al.*[162] In this work, lignin molecules are linked by PCL to form lignin-*graft*-PCL (Scheme 12). Lignin served as the initiator for the graft-from polymerization of PCL, followed by the synthesis of lignin-*graft*-PCL. Then, the hydroxyl terminus of PCL was functiona-

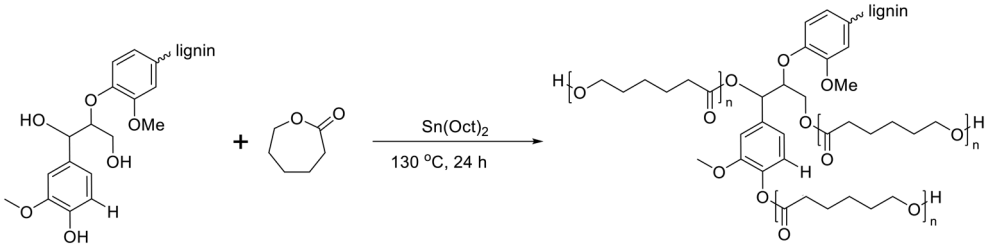

Scheme 9 Synthesis of lignin-*graft*-PCL using the graft-from method. Terminal β-O-4 softwood lignin unit is used for simplicity.

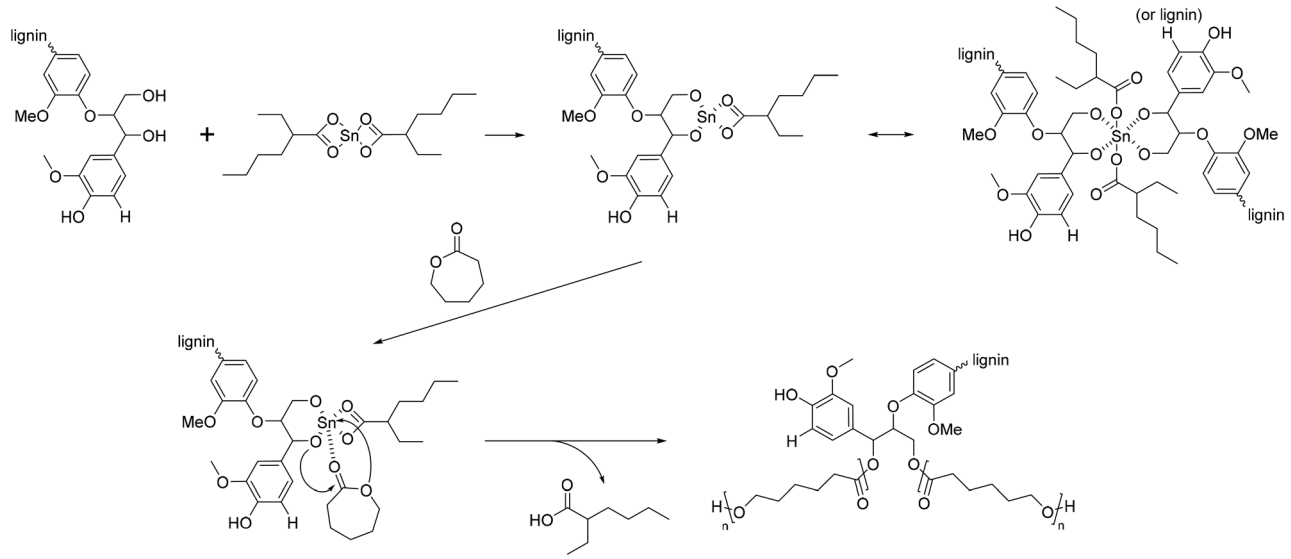

Scheme 10 Mechanism of ring-opening polymerization of caprolactone with $Sn(Oct)_2$. Terminal β-O-4 softwood lignin unit is used for simplicity.

lized as an alkyne group. Simultaneously, the hydroxyl group of the other natural lignin was reacted with bromobutyryl chloride by esterification and the bromo terminus was modified to become an azide terminus. The lignin-azide and lignin-*graft*-PCL-alkyne were linked by click chemistry (Scheme 12).

In 2019, Liu *et al.* reported crosslinked lignin-*graft*-PCL, which was synthesized by a graft-onto method through a Ru-catalyzed photoredox thiol–ene reaction.[56] Lignin was modified to have an alkene terminus by esterification and PCL was prepared with pentaerythritol, a tetraol, as an initiator. The four hydroxyl terminal groups of four-armed PCL were modified to possess thiol terminal groups. The four-armed PCL-SH was reacted with lignin–alkene to make PCL-S-C-C-lignin *via* a photoredox thiol–ene reaction in the presence of $Ru(bpy)_3Cl_2$ catalyst and *p*-toluidine under blue light (Scheme 13).

Common applications of lignin-*graft*-PCL include as an additive in the PCL matrix,[119] as a replacement for PCL,[126] as an antioxidant for biomedical applications,[118] as a nucleating agent for PCL,[115] as a shape memory material,[56] for thermal energy storage,[127] separation,[128] to coat a metal surface,[124] and as a polyol for polyurethane synthesis.[129]

Park *et al.*[119] and Tian *et al.*[126] introduced lignin-*graft*-PCL as a component for blending with PCL. Separately synthesized lignin-*graft*-PCL was blended with the PCL matrix to enhance its mechanical properties. Compared to natural lignin, lignin-*graft*-PCL showed much better dispersity in PCL (Fig. 14). Also, lignin *graft*-PCL showed enhanced mechanical properties compared to PLA.

The antioxidant application of lignin-*graft*-PCL was reported by Wang *et al.*[118] Nanofibers of a mixture of lignin-*graft*-PCL and PCL were prepared by an electrospinning process (Fig. 15a and b). PCL10LP2 is a composite fiber with 10% lignin-*graft*-PCL (mass feed ratio of lignin : CL was 2 : 8) and PCL10LP4 is a composite fiber with 10% lignin-*graft*-PCL (mass feed ratio of lignin : CL was 4 : 6) in PCL. The nanofibers of lignin-*graft*-PCL/PCL mixture (PCL10LP4 and PCL10LP2) showed 95.7% and 43.2% free radical inhibition, respectively, whereas PCL showed only 11.5% (Fig. 15c and d). The addition of lignin copolymers to the composition improved the antioxidant activities of the nanofibers, with a higher amount of lignin copolymers leading to increased free radical inhibition. In addition, the nanofibers showed excellent biocompatibility. Neurofilaments, mainly found in cells of neuronal origin, showed almost double the growth rate on the lignin-*graft*-PCL/PCL nanofibers than on PCL fibers (Fig. 15e–g).

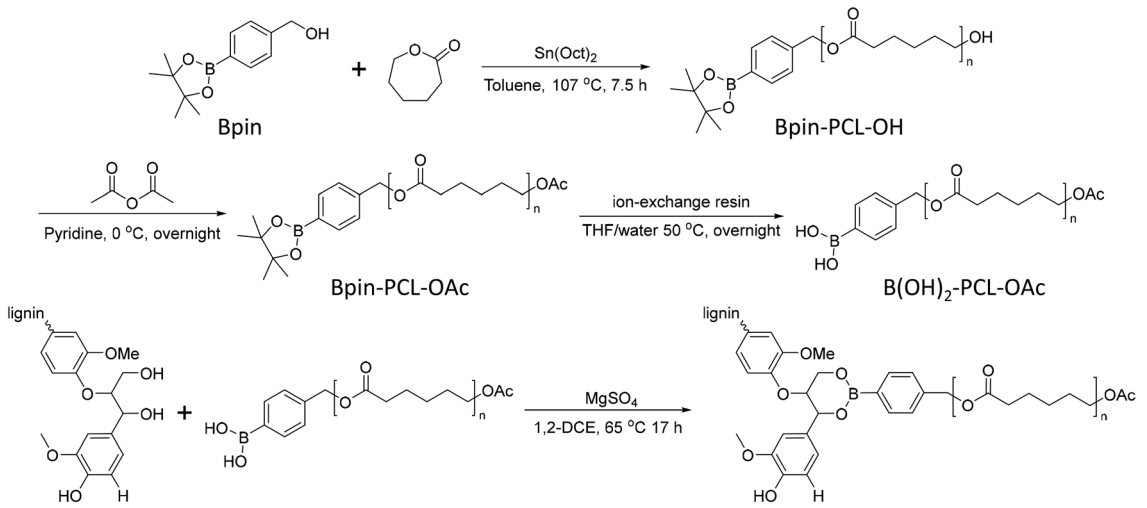

Scheme 11 Synthesis of separately prepared PCL and graft copolymerization of PCL onto lignin. Terminal β-O-4 softwood lignin unit is used for simplicity.

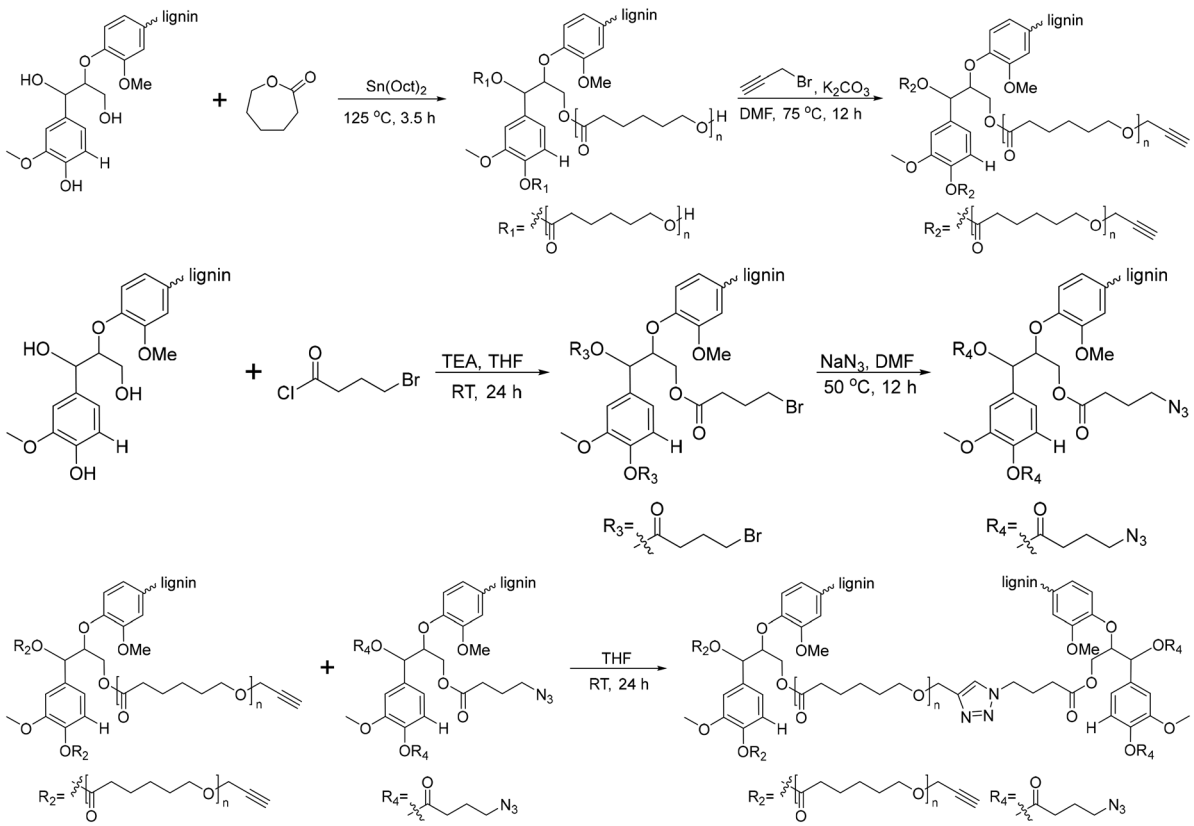

Scheme 12 Synthesis of lignin-*graft*-PCL by the graft-from method and lignin-*graft*-PCL-*graft*-lignin by the graft-onto method. Terminal β-O-4 softwood lignin unit is used for simplicity.

In 2015, Pérez-Camargo *et al.* reported the effect of lignin on the morphology, nucleation and crystallization kinetics of PCL using lignin-*graft*-PCL prepared by a graft-from method.[115] Lignin displayed a nucleating reaction in the PCL matrix to yield an intersecting lamellar structure. Especially at low contents (2–5 wt%) of lignin, a high efficiency value (close to 100%) of nucleation was observed. This led to an increase in crystallization and T_m as well as the isothermal crystallization rate of lignin-*graft*-PCL.

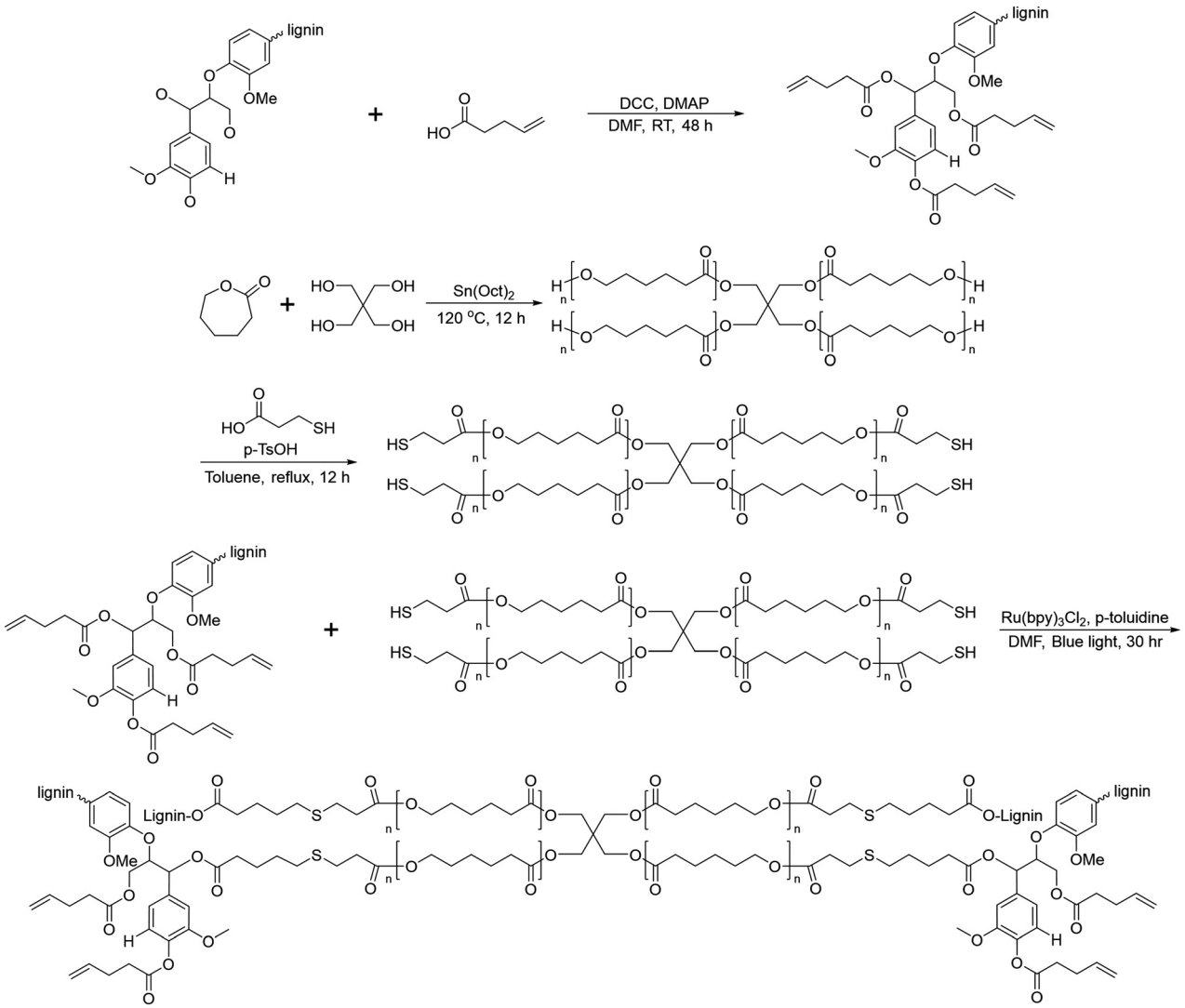

Scheme 13 Synthesis of lignin-*graft*-PCL by the graft-onto method using the thiol–ene reaction. Terminal β-O-4 softwood lignin unit is used for simplicity.

However, when the lignin content exceeds 18 wt%, antinucleation effects become apparent. The antinucleation effects refer to the inhibition of lignin on the crystallization process of PCL. This causes a decrease in both crystallization and T_m, reduces the degree of crystallinity, hinders annealing during thermal fractionation and significantly retards isothermal crystallization. The results can be explained by competition between the nucleating effects of lignin and intermolecular interactions caused by hydrogen bonding between PCL and lignin building blocks (Fig. 16).

Lignin-*graft*-PCL as a shape memory material was reported by Liu *et al.*[56] The shape memory mechanism of crosslinked polymers involves the interaction of net points and switching segments.[130–133]

Net points, formed through chemical and physical crosslinking, are essential for facilitating permanent shape recovery. On the other hand, switching segments exhibit distinct behaviors depending on the temperature.

The crosslinked lignin-*graft*-PCL was synthesized from lignin with 4-armed PCL with different weight % of lignin. Increased lignin amounts lead to higher gel contents and lower T_m and T_g. The prepared crosslinked lignin-*graft*-PCL showed an efficient and prompt thermal responsive shape memory function. Above T_{trans} (80 °C), the polymer exhibits enough chain flexibility for it to be deformed into a temporary shape under the application of an external force. Once the material is cooled below T_{cool} (10 °C), the temporary shape becomes solidified and is maintained at room temperature. When the material is reheated above T_{trans}, in the absence of an external force, it recovers its original shape, returning to its initial form (Fig. 17).

In 2022, Lee *et al.* reported the thermal energy storage function of lignin-*graft*-PCL.[127] Lee *et al.* prepared four different

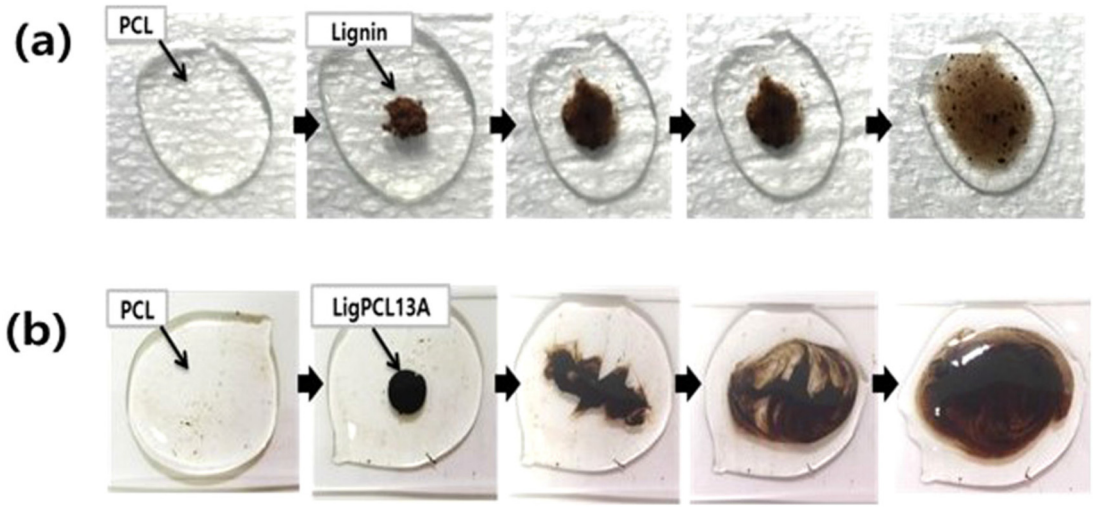

Fig. 14 Photographic images of melt mixing of PCL at 150 °C with (a) lignin and (b) lignin-*graft*-PCL. Reproduced from ref. 119 with permission from Springer Nature, copyright 2019.

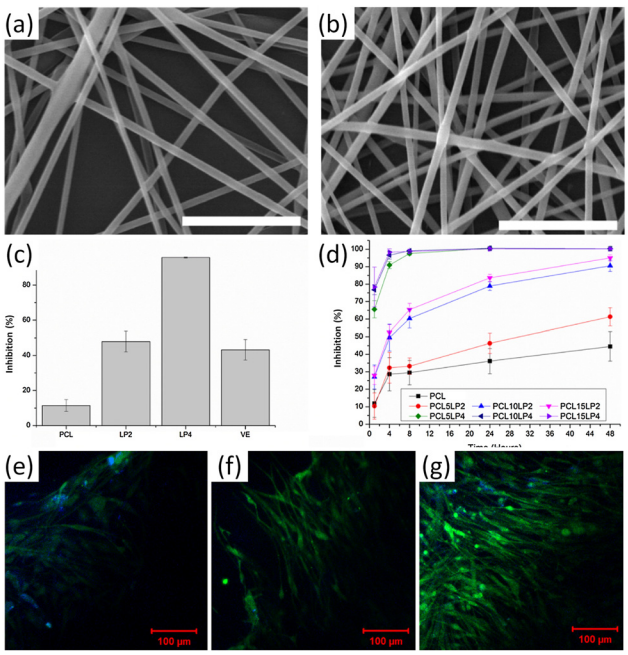

Fig. 15 (a and b) SEM images of different lignin-*g*-PCL nanofibrous scaffolds: (a) PCL10LP2, (b) PCL10LP4; (c) BMSC proliferation on different nanofibers; (d) Schwann cell proliferation on different nanofibers after H_2O_2 treatment; (e–g) MBP expression of Schwann cells on different nanofibers: (e) PCL, (f) PCL10LP2, (g) PCL10LP4. Green color: MBP; blue color: the nuclei. Reproduced from ref. 118 with permission from Elsevier, copyright 2018.

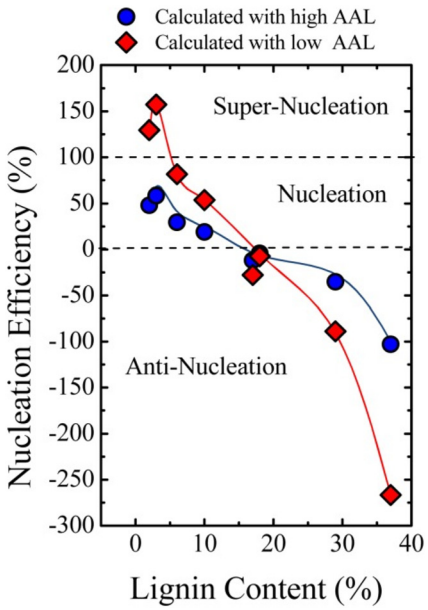

Fig. 16 Nucleation efficiency of lignin in PCL-*g*-lignin samples. The efficiency was calculated using reference crystallization parameters from both low average arm length (AAL) PCL and high AAL PCL. Reproduced from ref. 115 with permission from John Wiley and Sons, copyright 2015.

physically mixed samples with varying weight ratios, and prepared one lignin-*graft*-PCL (26 wt% lignin). The samples were prepared in a rectangular block on filter paper and exposed to a temperature beyond their T_m overnight. Then, the samples were removed from the filter paper, and the difference in weight from the initial state was measured. Fig. 18 shows the initial sample, the sample after heating, and leakage stains from melted block samples. The physically mixed samples (L4P6, L3P7, L2P8 and L1P9) melted and leaked as a gel upon exposure to high temperature, while lignin-*graft*-PCL retained its shape even at temperatures higher than its T_m. Also, leakage stains from melted block samples were observed after removing the samples from the filter paper. The leakage from lignin-*graft*-PCL on filter paper had the lowest weight, and a larger amount of lignin showed a lower leakage weight in the

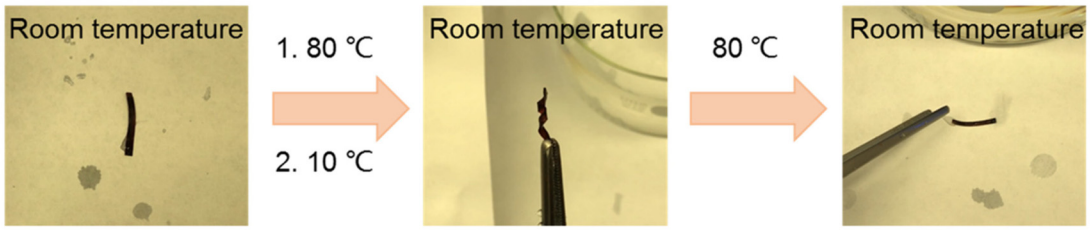

Fig. 17 Pictures of the shape memory behavior demonstrated by crosslinked lignin–PCL. The permanent shape (left) takes on the temporary shape (middle, shape change at 80 °C and then fixation at 10 °C) and is recovered again (right, shape recovery at 80 °C). All photos were taken at room temperature. Reproduced from ref. 56 with permission from John Wiley and Sons, copyright 2019.

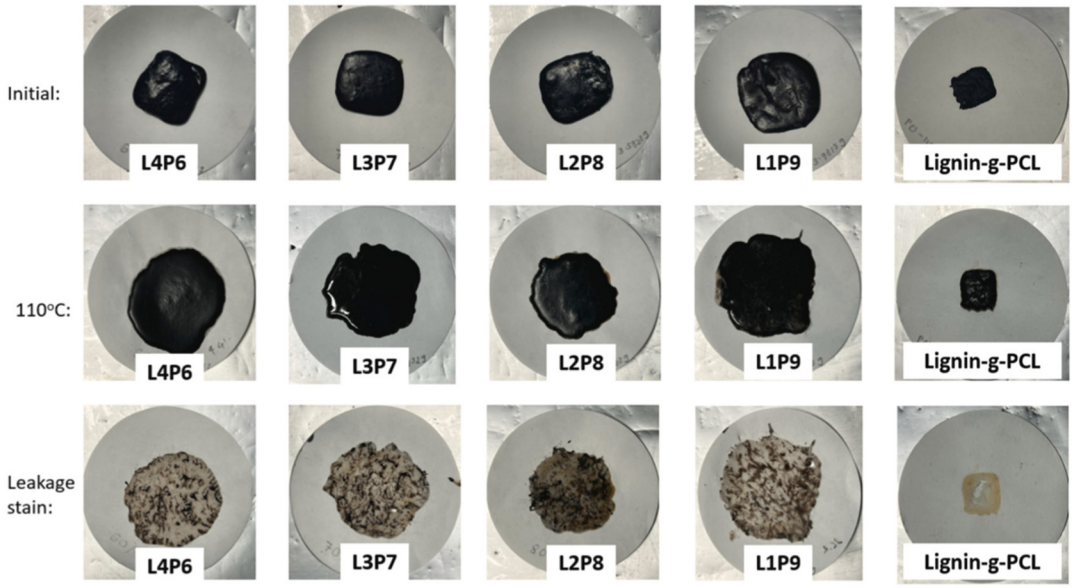

Fig. 18 Photographs taken during the leakage test at the initial stage, after high-temperature exposure and the leakage stain left on filter paper. Reproduced from ref. 127 with permission from Elsevier, copyright 2022.

physically mixed samples. This is because PCL is grafted to the lignin backbone, preventing leakage of the PCL as separate polymer components, as observed in the physically mixed samples.

The thermal response was investigated using IR imaging, as shown in Fig. 19b. Lignin-*graft*-PCL was placed on a heating module and heated to 80 °C, followed by waiting for 200 s for maximum thermal energy storage in the sample. Subsequently, the sample was cooled down to room temperature. The test results indicated a slow cooling process for lignin-*graft*-PCL, highlighting its potential as a heat storage material (Fig. 19b).

In 2022, Xie *et al.* reported the use of lignin-*graft*-PCL in a separation application.[128] In this work, lignin was copolymerized with caprolactone by solvent-free ring opening polymerization. Subsequently, filter paper was immersed in the solution of the synthesized lignin-*graft*-PCL for 12 h and then thoroughly dried. After that, SiO_2 (silicone oil) was dispersed on the sample as a second impregnation step. The organic solvent (chloroform, bottom phase, orange color in Fig. 20) and water (top phase and purple color in Fig. 20) mixture was added to the funnel and then passed through the prepared filter paper for separation. The separation efficiency (%) was calculated as the weight percentage of stopped water in the funnel over the originally added water in the mixture. The CFP-C (filter paper coated with lignin-*graft*-PCL) effectively filters low surface energy organic solvents into the vial, while retaining high surface energy water in the funnel. Lignin-*graft*-PCL's separation efficiency was 99.0%, whereas CFP-P (filter paper coated with homoPCL) showed only 12.8% due to the low hydrophobicity of the PCL coating. In the case of FP (uncoated filter paper), it filtered most of the water because of its hydrophilicity (Fig. 20).

Lignin graft copolymer as a coating agent on metal surfaces was reported in 2020 by Najarro *et al.*[124] The prepared lignin–PCL copolymer, which was synthesized by the graft-from method, was coated on a stainless steel surface. The lignin–PCL copolymer and cross-linker mixture served as the coating solution on the polished and rinsed steel. The author tested the adhesion properties and coating stability on the stainless-

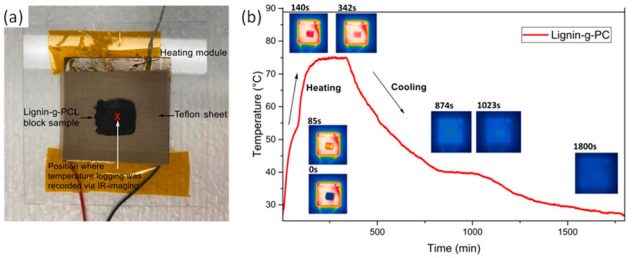

Fig. 19 (a) IR-imaging set-up and position of temperature logging, and (b) IR-imaging of lignin-*g*-PCL and its temperature profile over time for a block of lignin-*g*-PCL sample being heated beyond its melting temperature (~80 °C) and subsequently cooled. Reproduced from ref. 127 with permission from Elsevier, copyright 2022.

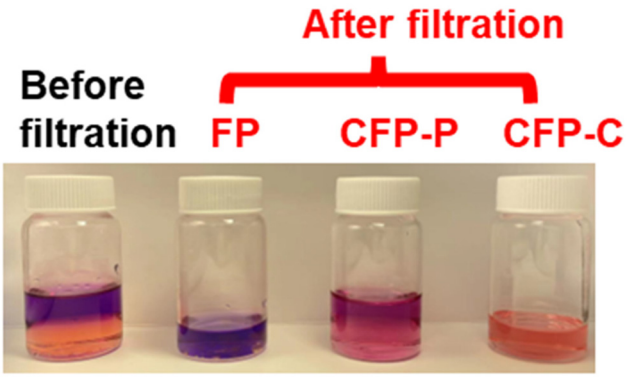

Fig. 20 Images of the original water (purple top layer)/chloroform (orange bottom layer) mixture and filtrates of FP, CFP-P, and CFP-C obtained. Reproduced from ref. 128 with permission from American Chemical Society, copyright 2022.

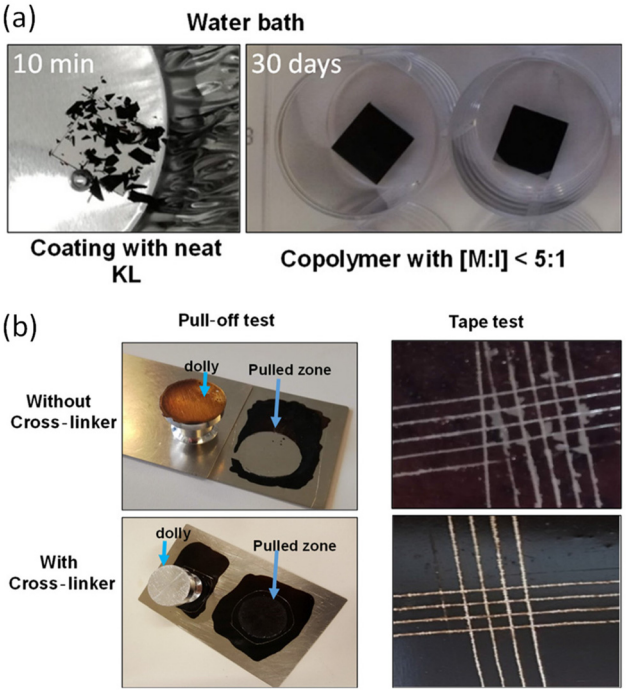

Fig. 21 (a) The stability test in a water bath at room temperature. (b) Pictures of adhesion tests for the lignin–PCL and lignin–PCL with cross-linker. Reproduced from ref. 124 with permission from American Chemical Society, copyright 2020.

steel surface. In a water bath, the coating with neat lignin showed clear differences from the coating with lignin–PCL copolymer. The neat lignin coating disintegrated in less than 10 min, whereas the coating with copolymers remained stable even after 30 days. This is attributed to the ester polymer arm from the copolymer enabling film formation, whereas neat lignin only exhibits rigidity without forming a film.

The crosslinker further enhanced the adhesion properties, which were measured by pull-off and cross-cut tape tests, by forming networks. The copolymer without crosslinker needs 0.6 MPa for pull-off adhesion tests and it showed only 1–2 on the scale for the cross-cut tape test. In this study, the results were evaluated using a 0–5 scale, where 5 indicates perfect adhesion. In contrast, the copolymer with crosslinker showed an adhesion force of 6.2 MPa for pull off and 4–5 on the scale for the cross-cut tape test (Fig. 21).

In 2017, Zhang *et al.* reported lignin-*graft*-PCL based polyurethane.[125] As shown in Scheme 14, PCL served as the soft segment along with hexamethylene diisocyanate (HDI). The lignin-*graft*-PCL containing polyurethane (LPU) was synthesized by the graft-onto method. In the first step of the synthesis procedure, the hydroxyl groups of lignin were activated by HDI, and then the PCL's hydroxyl groups reacted with isocyanate on activated lignin (top scheme in Scheme 14).

Several samples were prepared with different ratios of –NCO/OH and varying weight percentages of lignin/PCL to compare their mechanical properties. The LPU with a higher ratio of –NCO/OH showed improved mechanical properties, such as higher tensile strength, higher elongation break, and right-angle tear strength, because more isocyanate groups led to more cross-linking with hydroxyl groups. However, ratios of –NHC/OH higher than 1.75 resulted in decreased mechanical properties. The negative effect was caused by restricted movement of polymer chain segments due to increased cross-linking and enhanced intermolecular forces. Also, the polymer length of PCL affected LPU's properties. LPU with a lower molecular weight of PCL showed poorer mechanical properties because of a higher crosslinking density (shorter chain length between crosslinking points). The effect of the overall lignin content in the polymer was also examined. The tensile strength increased as the lignin content rose to 37.30%. However, a subsequent decrease occurred when the lignin content further increased from 37.30% to 43.15% because of excess lignin agglomeration.

4.3 Lignin-*graft*-poly(ethylene brassylate) (lignin-*graft*-PEB)

In 2021, Kim and Chung reported lignin-*graft*-poly(ethylene brassylate) (lignin-*graft*-PEB).[134] Lignin was chemically modified by sebacic acid to introduce a carboxylic acid functionality into the hydroxyl group of lignin. Another precursor of the

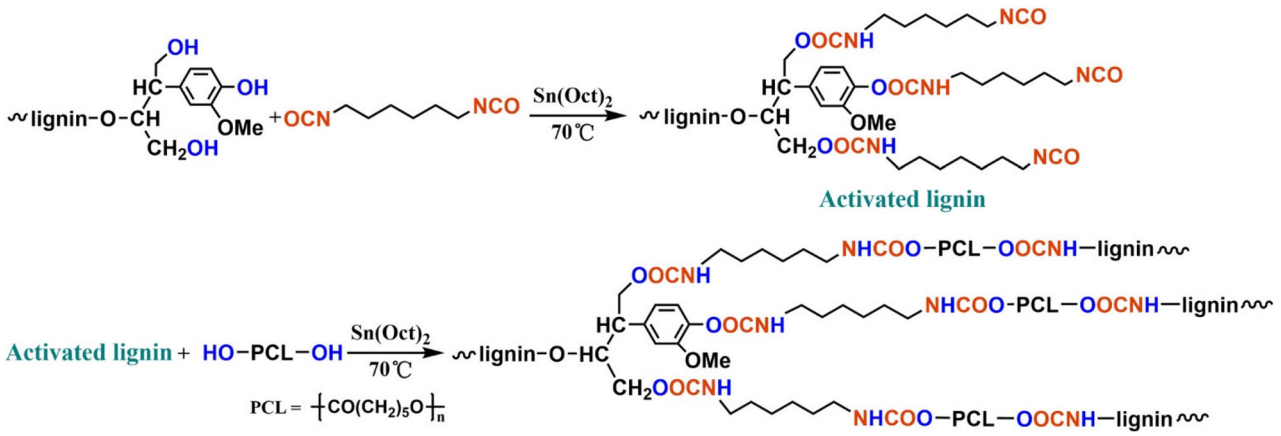

Scheme 14 Synthesis route to the lignin–PCL based polyurethane. Reproduced from ref. 125 with permission from American Chemical Society, copyright 2017.

copolymer, PEB, was prepared by ring-opening polymerization of ethylene brassylate in the presence of the 1,5,7-triazabicyclo [4.4.0]dec-5-ene (TBD) catalyst without another initiator. The condensation copolymerization of the modified lignin and PEB occurred by the reaction between the TBD terminus of PEB and the carboxylic acid of the modified lignin (Scheme 15). The thermal properties of lignin-*graft*-PEB exhibit high stability, with a T_m of 78 °C and a T_g of 12 °C. Mechanical property tests reveal that lignin-*graft*-PEB possesses comparable properties to commercial polyolefins such as LDPE, with a tensile strength of 7.34 MPa and a Young's modulus of 442.9 MPa, surpassing that of LDPE. The crucial factors influencing the mechanical properties include the lignin/PEB ratio and the molecular weight of PEB, as identified through comprehensive property tests. Especially, the presence of covalent bond linkages between lignin and PEB is essential for achieving enhanced mechanical properties, emphasizing the significance of their chemical integration.

4.4 Lignin-*graft*-poly(hydroxybutyrate) (lignin-*graft*-PHB)

Poly(3-hydroxybutyrate) (P3HB) stands out as the first isolated and characterized polymer within the polyhydroxyalkanoate (PHA) family. P3HB possesses a highly crystalline structure due to its linear chain configuration.[135] Three primary methods for producing PHB are available. The first involves the ring opening polymerization of β-butyrolactone.[136–138] Another method utilizes natural or transgenic plants, capable of synthesizing PHAs in their cells due to the abundance of

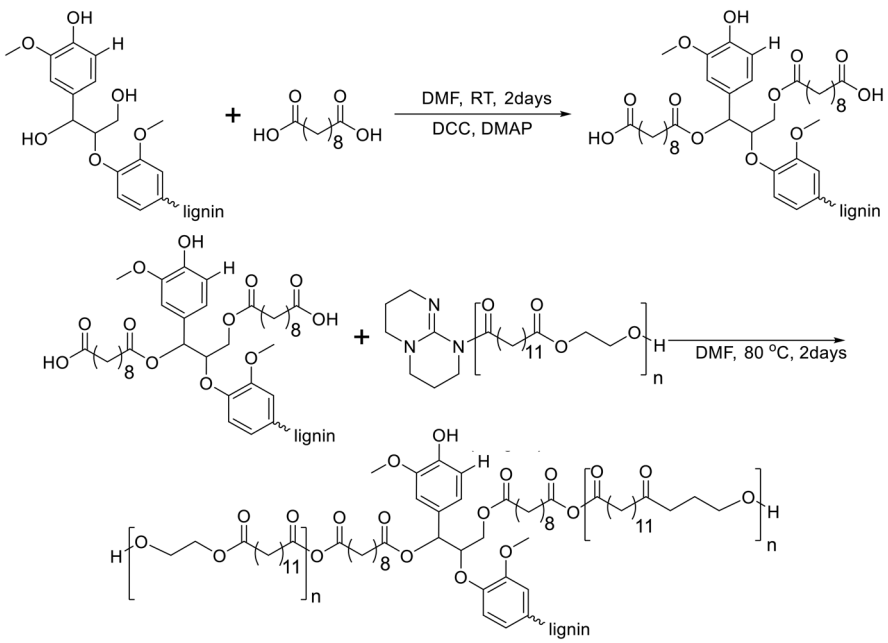

Scheme 15 Synthesis of lignin-*graft*-poly(ethylene brassylate). Terminal β-O-4 softwood lignin unit is used for simplicity.

acetyl-CoA, a key substrate in PHA biosynthesis. Examples include *Linum usitatissimum* L., commonly known as flax.[139] The third method entails bacterial fermentation, where optimal conditions can yield PHA materials constituting over 90% of the cell's dry weight.[140] This bacterial fermentation approach is the one most widely employed for PHB synthesis.

Lignin-*graft*-PHB was reported by Kai *et al.* in 2019.[141] Lignin-*graft*-PHB was synthesized by a graft-from method with lignin and butyrolactone without solvent. $Sn(Oct)_2$ served as a catalyst; it is commonly employed in ring opening polymerizations (Scheme 16). The prepared lignin-*graft*-PHB was used to produce nanofibers by electrospinning with PHB. The prepared lignin-*graft*-PHB/PHB nanofibers were tested for their mechanical properties, antioxidant ability, and biocompatibility. Only 2% of such a copolymer is required to increase the tensile strength by ~4 times, stiffness by 1.5 times, and elongation by ~10 times compared to pure PHB. Increasing the lignin content to 5% resulted in improved mechanical properties; however, beyond 5%, enhancements decreased due to the brittle nature of lignin (Fig. 22a). Furthermore, lignin-*graft*-PHB/PHB nanofibers display tunable antioxidant activity and good biocompatibility both *in vitro* and *in vivo*. Especially, higher lignin contents showed a higher antioxidant ability (Fig. 22b–h). These properties indicate that lignin-*graft*-PHB can have broader applications in the biomedical field.

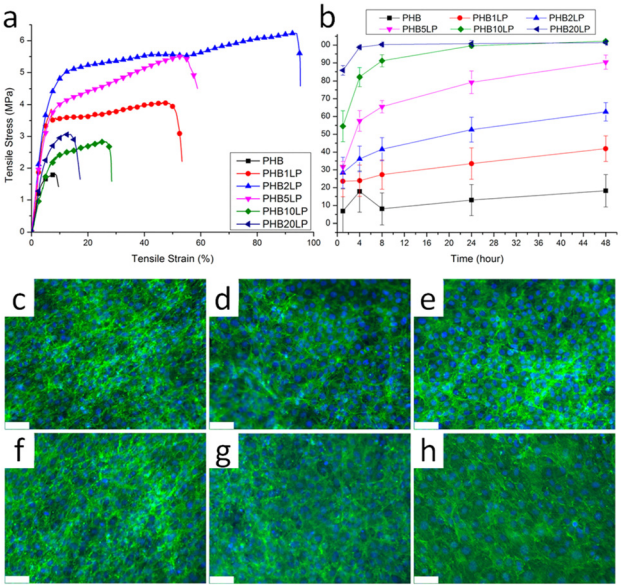

Fig. 22 (a) Typical tensile stress–strain curves of PHB and PHB/lignin–PHB nanofibers. (b) Antioxidant activity of PHB/lignin–PHB nanofibers (DPPH assay). (c–h) NIH-3T3 fibroblasts stained with DAPI and phalloidin after 8 days of culture on various nanofibers: (c) PHB, (d) PHB1LP, (e) PHB2LP, (f) PHB5LP, (g) PHB10LP, and (h) PHB20LP nanofibers (scale bar = 75 μm). The tight mesh of cells after 8 days of culture indicates very high confluency and good biocompatibility. Reproduced from ref. 141 with permission from American Chemical Society, copyright 2019.

4.5 Lignin-*graft*-poly(caprolactone-*co*-lactic acid) (lignin-*graft*-PCLLA)

Lignin can undergo graft copolymerization not only with a single polyester but also with copolymers such as poly(caprolactone-*co*-lactic acid) (PCLLA).[142–144]

Sun *et al.* reported lignin-*graft*-PCLLA synthesized by a graft-from method in 2015 (Scheme 17a).[142] PCLLA was polymerized by ring opening polymerization, initiated by the hydroxyl group on lignin in toluene solvent. Then, separately synthesized PDLA was polymerized onto the prepared lignin-*graft*-PCLLA to use it as a compatibilizer. Lignin-*graft*-PCLLA-PDLA provides a strong filler–matrix interfacial attraction, even improving the dispersity of polymers in the matrix. In addition, lignin-*graft*-PCLLA-PDLA has a role as a reinforcement agent in PLLA blend, resulting in improved mechanical properties compared to pure PLLA.

In 2017, Kai *et al.* introduced the solvent-free synthesis of lignin-*graft*-PCLLA (Scheme 17b).[143] The synthesized lignin-*graft*-PCLLA acts as an additive for both PCL and PLLA, to prepare uniform nanofibers *via* electrospinning (Fig. 23). The mechanical properties and antioxidant effects of these fibers were investigated. The blend of lignin-*graft*-PCLLA in PCL matrix reinforced the PCL nanofibers. In addition, the multi-polymer blend of lignin-*graft*-PCLLA/PCL/PLA blend nanofibers exhibited good antioxidant activity and biocompatibility. This outcome highlights the potential of lignin-*graft*-PCLLA/PLA and lignin-*graft*-PCLLA/PCL blends as materials for biomedical applications.

4.6 Lignin-*graft*-poly(3-hydroxybutyrate-*co*-3-hydroxyvalerate) (lignin-*graft*-PHBV)

Poly(3-hydroxybutyrate-*co*-3-hydroxyvalerate) is commonly named poly(3-hydroxybutyric acid-*co*-3-hydroxyvaleric acid) (PHBV). PHBV is copolymerized with PHB and 3-hydroxyvale-

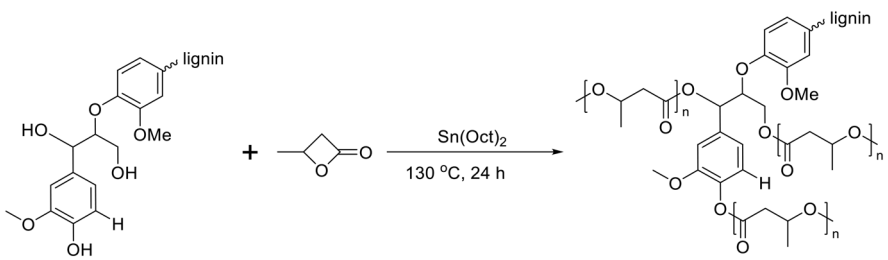

Scheme 16 Synthesis of lignin-*graft*-poly(3-hydroxybutyrate). Terminal β-O-4 softwood lignin unit is used for simplicity.

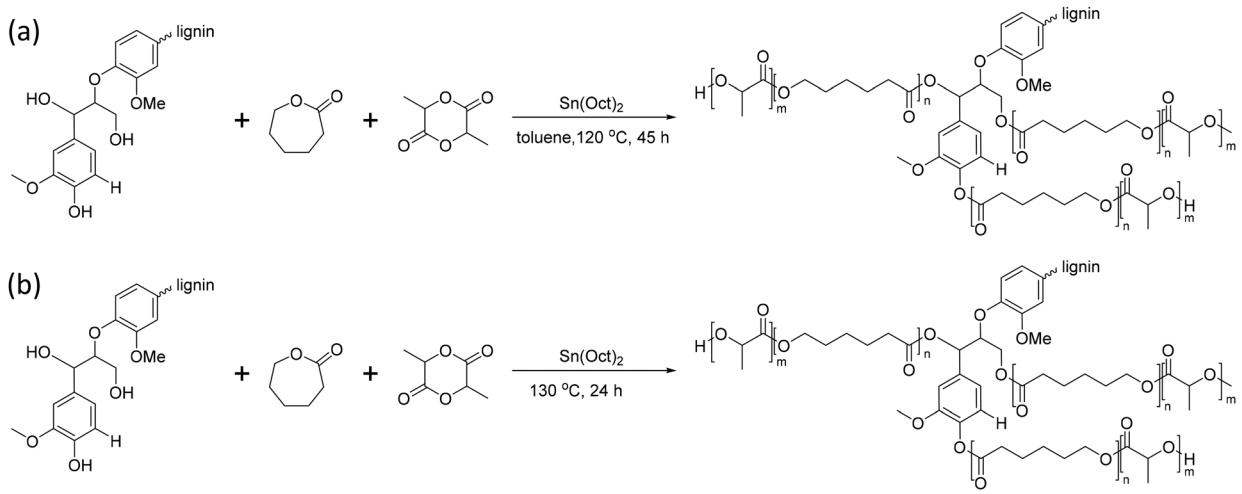

Scheme 17 Synthesis of lignin-*graft*-PCLLA through the graft-from method (a) with toluene as a solvent and (b) without solvent. Terminal β-O-4 softwood lignin unit is used for simplicity.

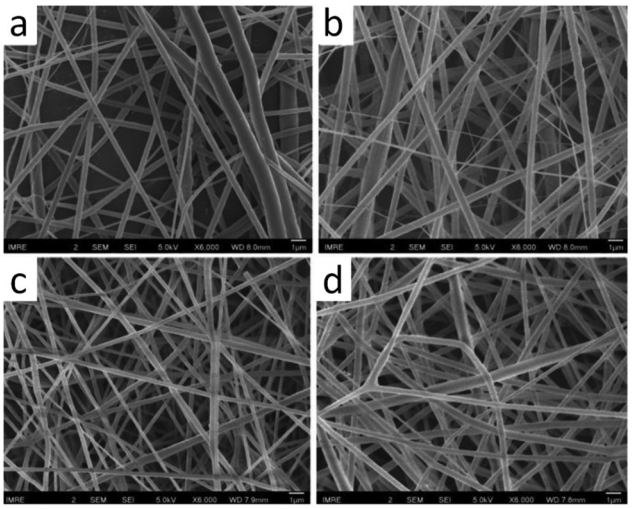

Fig. 23 SEM images of electrospun (a) PCL, (b) PCL/LP1, (c) PLLA, and (d) PLLA/LP1 nanofibers. Scale bars = 1 μm. Reproduced from ref. 143 with permission from American Chemical Society, copyright 2017.

rate (HV) units in a bacterial fermentation process, aiming to increase flexibility and to decrease T_m for easier processing.[145] The T_m of PHBV is lower than that of PHB and diminishes with an increased fraction of HV in the polymer, thereby widening the processing range and results in an improvement in the ductility and flexibility of the polymer.[146] PHBV also exhibits resistance to hydrolysis and better resilience to ultraviolet radiation.[147–149] Consequently, PHBV has attracted considerable attention from various research groups due to its high flexibility/strength and reduced chain packing/toughness.[150–153] Moreover, the increased proportion of HV within the PHB matrix make the overall polymer more amorphous, which is advantageous for drug release. Drugs typically exhibit easier diffusion through the amorphous region of a polymer.[154]

In 2016, Luo *et al.* reported lignin-*graft*-PHBV, as shown in Scheme 18.[155] Lignin-*graft*-PHBV was prepared by a graft-onto method to improve the interfacial adhesion of lignin and PHBV. In the first step of polymerization, a radical initiator, dicumyl peroxide (DCP), was added to lignin and PHBV to

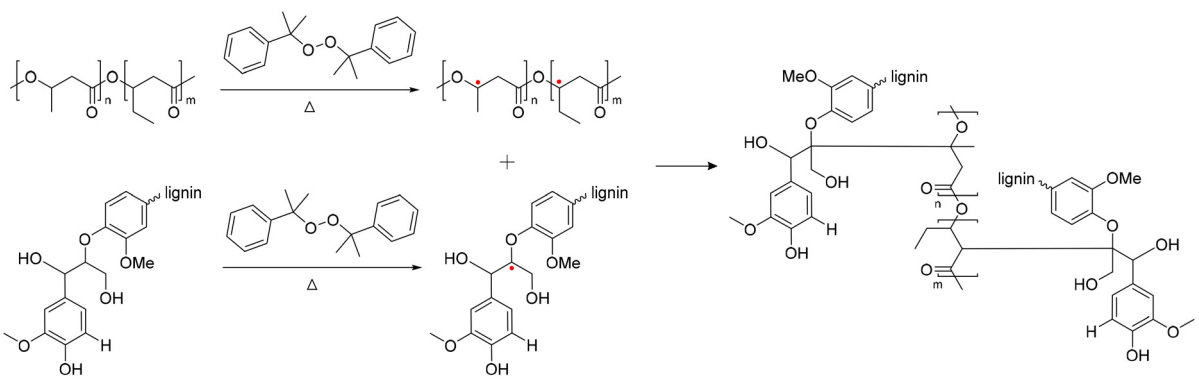

Scheme 18 Synthesis of lignin-*graft*-PHBV. Terminal β-O-4 softwood lignin unit is used for simplicity.

form radicals during melt extrusion. The generated radicals lead to covalent bond grafting (Scheme 18). Four different types of lignin-*graft*-PHBV were prepared with different amounts of radical initiator. The mechanical properties of those prepared lignin-*graft*-PHBV samples were studied. Lignin-*graft*-PHBV showed a higher modulus but a lower strain at break compared to homo PHBV. This can be attributed to the presence of lignin, a rigid three-dimensional macromolecule, which restricts chain movement during deformation. In particular, lignin-*graft*-PHBV, which was linked with 2% radical initiator, exhibited significantly enhanced mechanical properties, a higher modulus, and a higher tensile strength and strain at break, compared to the blend of lignin and PHBV. According to the spherulite morphology study, pure PHBV had an average radius of approximately 700 μm of spherulites. Crosslinked PHBV showed similar spherulites, but the size was substantially decreased to 220 μm. On the other hand, lignin-*graft*-PHBV showed a smaller size and significantly higher number of spherulites compared to both PHBV and crosslinked PHBV. The grafting point between PHBV and lignin likely served as a nucleation site. The increased number of grafting points hindered diffusion, resulting in a higher concentration of radical initiator regionally, leading to a larger number of smaller spherulites (Fig. 24).

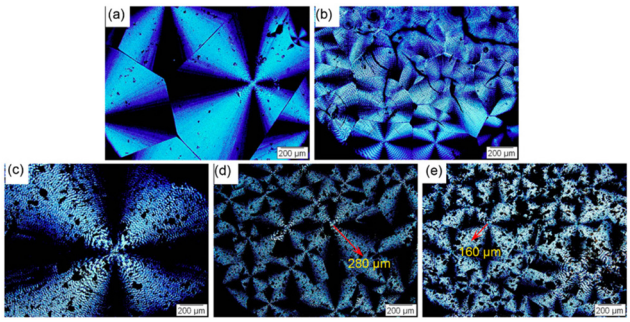

Fig. 24 Micrographs of (a) PHBV, (b) crosslinked PHBV, (c) PHBV–lignin blend, (d) PHBV-1-lignin with 1% DCP, and (e) PHBV-2-lignin with 1% DCP crystallized at 90 °C. Scale bar: 200 μm. Reproduced from ref. 155 with permission from American Chemical Society, copyright 2016.

4.7 Lignin-*graft*-poly(caprolactone)-poly(hydroxybutyrate) (lignin-*graft*-PCL-PHB)

In 2018, Kai *et al.* reported lignin-*graft*-PCL-PHBs and investigated their role as a filler of PHB nanofibers.[156] The lignin copolymers are synthesized by solvent-free ring-opening polymerization of butyrolactone and caprolactone in the presence of a tin catalyst. They prepared lignin-*graft*-PHB (LPH), lignin-*graft*-random copolymer of PHB and PCL (LPHC), lignin-*graft*-PHV-PCL (LPH + C), and lignin-*graft*-PCL-PHB (LPC

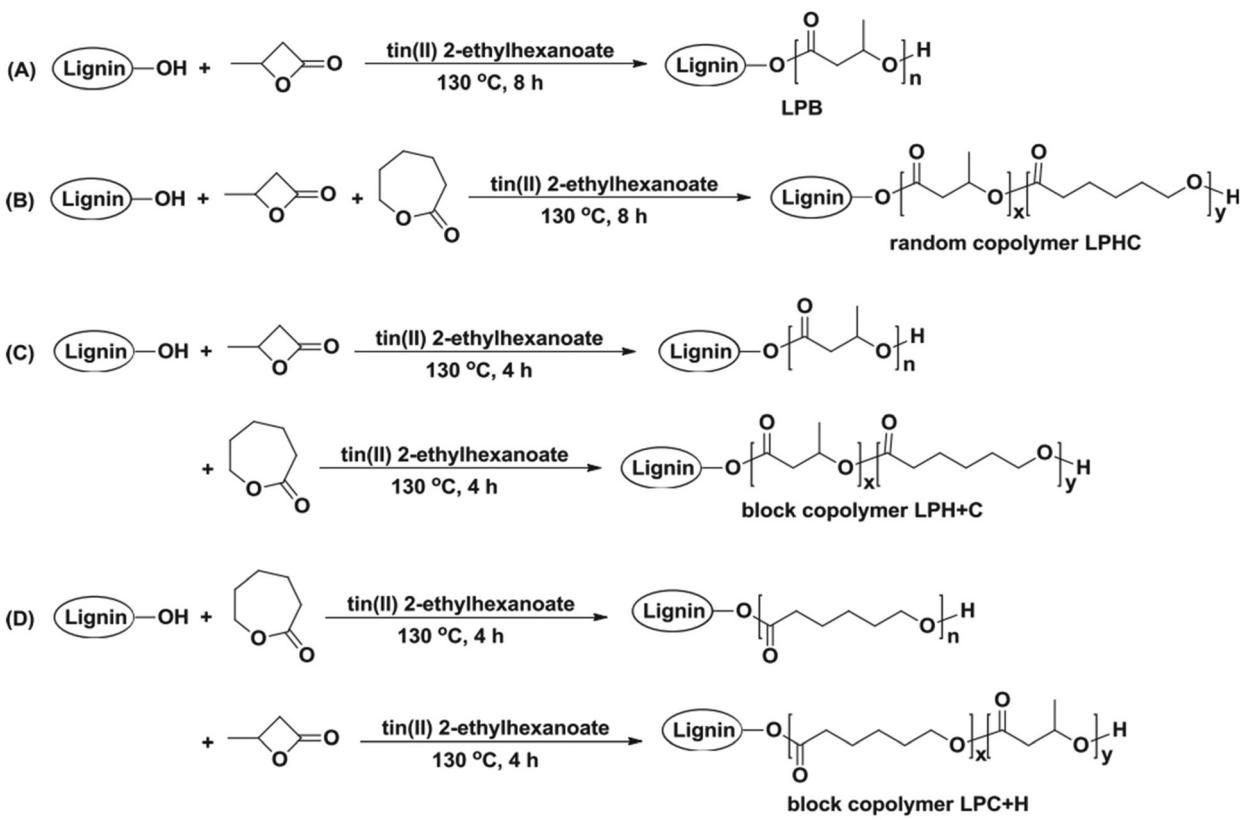

Scheme 19 The synthetic routes to lignin PHB copolymers: (A) lignin-*graft*-PHB (LPB), (B) lignin-*graft*-random copolymer of PHB and PCL (LPHC), (C) lignin-*graft*-PHV-PCL (LPH + C) and (D) block copolymer lignin-*graft*-PCL-PHB (LPC + H). Reproduced from ref. 156 with permission from Elsevier, copyright 2018.

+ H) (Scheme 19). Then, these lignin copolymers are mixed with PHB at a mass ratio of 5% and produce nanofibers through electrospinning. The PHB nanofibers showed a tensile strength of 1.81 MPa, a modulus of 80.9 MPa, and an elongation at break of 15%. The addition of LPH decreased the tensile strength and Young's modulus, while the elongation at break was increased. The addition of LPHC also resulted in decreased strength and modulus; additionally, it showed a decreased elongation at break. The nanofibers that consisted of PHB and LPH + C showed an enhanced tensile strength and modulus, while they showed the smallest value of elongation at break of 8%. The addition of LPC + H exhibited the best enhancement of the mechanical properties, the highest tensile strength, Young's modulus, and elongation at break. These results indicated that lignin acted as a rigid core for nanofibers, and PCL segments acted as a rubber phase between the PHB matrix and lignin core. Also, the PHB blocks improve the interaction between the lignin copolymer and PHB matrix. Thus, the addition of LPC + H showed the best performance due to the PHP outer segments of LPC + H mostly enhancing the interaction with the PHP matrix (Fig. 25).

4.8 Lignin-*graft*-polyester/amide

In 2021, a graft copolymer with lignin and polyester/amide consisting of a short-chain diacid (succinic acid, adipic acid, and suberic acid), butanediol, and diamino butane was reported by Young *et al.* as shown in Scheme 20.[157] The study aimed to develop fully biobased thermoplastic lignin copolymers using a two-step, solvent-free melt condensation process. The first step involved creating a low-molecular-weight prepolymer from butanediol (BD), diaminobutane (DAB), and one of three diacids: succinic acid (SA), adipic acid (AA), or suberic acid (SuA). These prepolymers were designed to terminate predominantly with carboxylic acid functionalities. In the second step, the prepolymers were reacted with softwood kraft lignin to form lignin–copolyester/amides. The study monitored the progression of polymerization using FTIR spectroscopy and characterized the resulting lignin copolymers' mechanical, thermal, and structural properties. These copolymers demonstrated thermoplastic behavior and varied tensile properties based on their diacid chain length, lignin content, and DAB content, showing potential for creating sustainable, biobased thermoplastic materials.

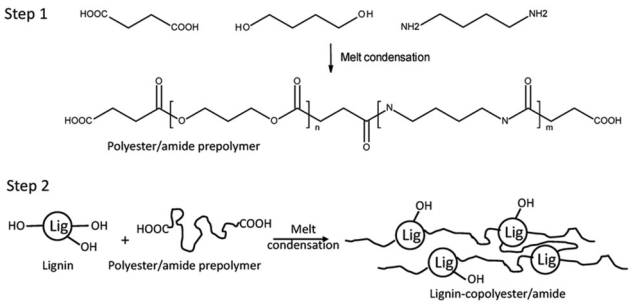

Scheme 20 Schematic showing the 2-step process for producing the polybutylene–succinate/succinamide prepolymer and lignin–copolyester/amides (lignin–copolybutylene–succinate/succinamide). Reproduced from ref. 157 with permission from MDPI, copyright 2021.

The synthesized lignin–copolyester/amides were found to have semi-crystalline structures with properties influenced by their composition. The succinic acid-based copolymers were stiff and brittle, while adipic acid-based ones were more flexible, and suberic acid-based copolymers displayed intermediate characteristics. Furthermore, lignin contents above 30% hindered the melt behavior, suggesting a limit for practical applications.

4.9 Summary

In this section, we discussed lignin-*graft*-polyesters. The copolymers are synthesized by either graft-from or graft-onto methods. Ring-opening polymerization is usually used for the graft-from method. Polycondensation, the thiol–ene reaction, azide–alkyne click chemistry, and radical reactions are used for the graft-onto method. Lignin copolymers have diverse applications across several fields due to their unique properties and the benefits they confer when combined with other polymers. The common applications of lignin-*graft*-polyesters include as additives to achieve higher mechanical properties, improved thermal stability, greater dispersity, and antioxidant applications. These benefits result from lignin's high mechanical properties (such as high Young's modulus, strain at break, and tensile strength), high glass transition temperature, and antioxidant properties.

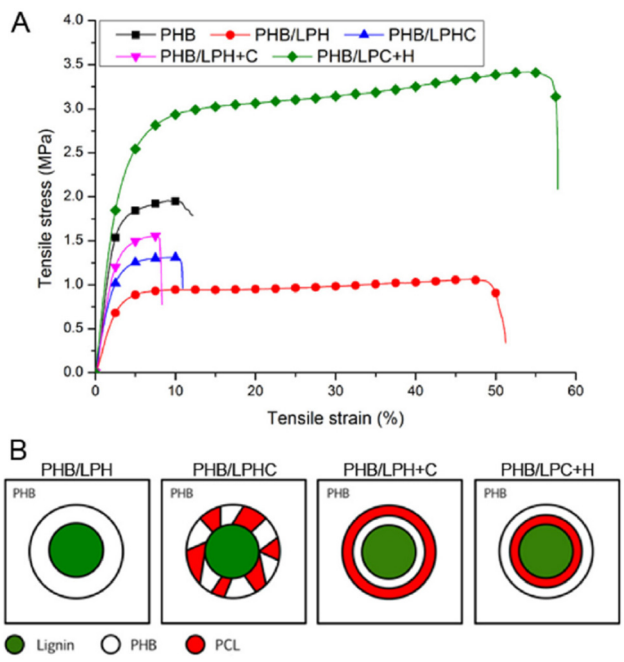

Fig. 25 (A) Typical stress–strain curves of electrospun nanofibers obtained from a tensile test. (B) Proposed dispersion models to show how different lignin copolymers disperse in PHB matrix. Reproduced from ref. 156 with permission from Elsevier, copyright 2018.

One prominent example is lignin-*graft*-polycaprolactone (lignin-*graft*-PCL). These materials are widely used as additives in PCL matrices to enhance the mechanical properties, providing improvements in flexibility, strength, and durability. They serve as a replacement for PCL, offering a cost-effective and environmentally friendly alternative. Additionally, lignin-*graft*-PCL copolymers act as antioxidants, making them suitable for biomedical applications where oxidative stress needs to be minimized. They are also used as nucleating agents for PCL, aiding in the crystallization process and improving the material's overall properties. These properties are affected by lignin's free volume due to its bulk polymer size. Moreover, lignin-*graft*-PCL copolymers have applications in shape memory materials, which can return to their original shape after deformation when exposed to an external stimulus like heat. They are also utilized in thermal energy storage systems due to their capacity to absorb and release heat efficiently. In separation processes, these copolymers are employed for their excellent barrier properties, making them suitable for filtration and purification applications. Additionally, they are used to coat metal surfaces to enhance corrosion resistance and provide a protective layer. In the field of polyurethane synthesis, lignin-*graft*-PCL copolymers serve as polyols, contributing to the creation of foams, adhesives, and elastomers with improved mechanical and thermal properties.

In the realm of biomaterials, lignin copolymers such as lignin-*graft*-polyhydroxybutyrate (lignin-*graft*-PHB) show significant promise. These copolymers can be processed into nanofibers through electrospinning, a technique that produces fibers with enhanced mechanical properties, antioxidant activity, and biocompatibility. When incorporated into materials, even in small amounts, lignin-*graft*-PHB copolymers can significantly improve tensile strength, stiffness, and elongation, making them ideal for medical devices, tissue engineering, and other biomedical applications. The incorporation of lignin-*graft* copolymers can increase tensile strength by up to four times, stiffness by 1.5 times, and elongation by ten times, demonstrating their potential to create more durable and versatile biomaterials. These applications highlight the versatility and potential of lignin copolymers for creating sustainable, high-performance materials for various industrial and biomedical uses.

5. Limitation of lignin-*graft*-polyesters

Lignin-*graft*-polyesters have emerged as promising alternatives in the quest for sustainable materials, leveraging lignin's abundance and eco-friendly attributes. Despite their potential, these copolymers encounter challenges that hinder their widespread adoption in industrial applications.

One primary hurdle is the structural complexity of lignin itself. As a natural polymer with a complex molecular structure, achieving a uniform dispersion within polymer matrices remains elusive. This complexity often results in heterogeneous material properties, limiting consistency and reliability in mechanical performance.

Moreover, the reactivity of lignin during polymerization poses challenges. While lignin offers diverse chemical functionalities, ensuring reproducible reactions in a controlled manner proves difficult. This unpredictability can lead to undesirable side reactions, further complicating the manufacturing process and affecting material quality.

In terms of physical properties, some lignin-*graft*-polyesters exhibit lower mechanical characteristics compared to traditional polymers (*e.g.*, PET, HDPE, and PP). Factors such as reduced strength, hardness, and elongation diminish their suitability for applications requiring robust and high-performance materials. Additionally, lignin's susceptibility to thermal degradation and its high viscosity during processing present obstacles to achieving efficient manufacturing and product consistency.

Aesthetic considerations also play a crucial role in the market acceptance of lignin-*graft*-polyesters. The inherent dark color of lignin often compromises the desired appearance of the final products, limiting their appeal in consumer-oriented industries where visual appeal is paramount. Generally, white or transparent polymers have much broader applications in industry.

From an economic perspective, the extraction and purification of lignin are resource-intensive processes, adding to production costs. This economic barrier, coupled with the competitive pricing of established polymer alternatives such as petroleum-based polyolefins, challenges the commercial viability of lignin-*graft*-polyesters.

Furthermore, despite being sourced from renewable biomass, environmental concerns persist. Although the actual amount is not large, the synthesis processes for lignin-*graft*-polyesters may involve chemicals that raise ecological questions. The unavoidable use of such chemicals is gradually being addressed by developing less environmentally harmful solvents and catalyst systems to perform the same types of chemical reactions that previously required ordinary organic solvents and chemicals.

In conclusion, while lignin-*graft*-polyester hold promise as sustainable materials, their adoption faces multifaceted challenges, ranging from structural complexities and reactivity issues to economic viability and environmental considerations. Overcoming these obstacles demands continued research efforts aimed at refining processing techniques, enhancing material properties, and ensuring environmental sustainability for broader applications in industrial sectors.

6. Conclusions

This review discusses the synthesis and applications of biodegradable lignin-*graft*-polyesters. Emphasizing graft copolymerization as an efficient method to seamlessly integrate lignin with other aliphatic polyesters, the study focuses on naturally biodegradable polyesters, with the majority of raw

materials sourced from biomass. Beyond their intrinsic sustainability, these lignin-*graft*-polyesters benefit from lignin, providing mechanical strength, enhanced hydrophobicity and aromaticity, and as a non-food resource. The reviewed polyesters, including PLA, PGA, PCL, PEB, and PHA, and their diverse copolymers, showcase the versatility of lignin-based graft copolymer synthesis. The multitude of presented chemical reaction schemes offers a valuable guide to understanding recent trends in lignin and polyester copolymerization. Apart from synthesis, the review explores the properties and applications of these lignin-*graft*-polyesters, offering fundamental insights for detailed structure–property relationship studies in closely related biomass-based degradable polymers. The comprehensive examination of these materials not only adds to our understanding of their potential but also positions them as solutions to environmental challenges, with broad applicability across various industrial sectors. This review thus serves as a valuable resource, providing a holistic perspective on biodegradable lignin-*graft*-polyesters, from synthesis methodologies to their diverse applications and potential environmental contributions.

Data availability

No primary research results, software, or code have been included, and no new data were generated or analyzed as part of this review.

Conflicts of interest

There are no conflicts to declare.

Acknowledgements

This project was funded at least in part with federal funds awarded to the State of Florida from the United States Department of Agriculture National Institute of Food and Agriculture (Award #2019-70007-30368).

References

1 J. A. Van Franeker and K. L. Law, *Environ. Pollut.*, 2015, **203**, 89–96.
2 I. Kyrikou and D. Briassoulis, *J. Polym. Environ.*, 2007, **15**, 125–150.
3 K. L. Law, N. Starr, T. R. Siegler, J. R. Jambeck, N. J. Mallos and G. H. Leonard, *Sci. Adv.*, 2020, **6**(44), DOI: **10.1126/sciadv.abd0288**.
4 A.-C. C. Albertsson and M. Hakkarainen, *Science*, 2017, **358**, 872–873.
5 EUPB, European Bioplastics. What are Bioplastics?, **https://docs.european-bioplastics.org/2016/publications/fs/EUBP_fs_what_are_bioplastics.pdf**.
6 C. Matthews, F. Moran and A. K. Jaiswal, *J. Cleaner Prod.*, 2021, **283**, 125263.
7 R. Meys, A. Kätelhön, M. Bachmann, B. Winter, C. Zibunas, S. Suh and A. Bardow, *Science*, 2021, **374**, 71–76.
8 M. H. Rahman and P. R. Bhoi, *J. Cleaner Prod.*, 2021, **294**, 126218.
9 T. J. Gutiérrez, *Composites Materials for Food Packaging*, Wiley, 2018, pp. 269–296.
10 J. H. Song, R. J. Murphy, R. Narayan and G. B. H. Davies, *Philos. Trans. R. Soc., B*, 2009, **364**, 2127–2139.
11 N. A. A. B. Taib, M. R. Rahman, D. Huda, K. K. Kuok, S. Hamdan, M. K. B. Bakri, M. R. M. B. Julaihi and A. Khan, *Polym. Bull.*, 2023, **80**, 1179–1213.
12 N. K. Kalita, N. A. Damare, D. Hazarika, P. Bhagabati, A. Kalamdhad and V. Katiyar, *Environ. Challenges*, 2021, **3**, 100067.
13 P. T. Martone, J. M. Estevez, F. Lu, K. Ruel, M. W. Denny, C. Somerville and J. Ralph, *Curr. Biol.*, 2009, **19**, 169–175.
14 H.-R. Bjørsvik and F. Minisci, *Org. Process Res. Dev.*, 1999, **3**, 330–340.
15 K. V. Sarkanen and C. H. Ludwig, *Lignins: occurrence, formation, structure and reactions*, Wiley-Interscience, New York, 1971.
16 W. Boerjan, J. Ralph and M. Baucher, *Annu. Rev. Plant Biol.*, 2003, **54**, 519–546.
17 D. Kai, M. J. Tan, P. L. Chee, Y. K. Chua, Y. L. Yap and X. J. Loh, *Green Chem.*, 2016, **18**, 1175.
18 C. J. L. Constantino, A. Dhanabalan, A. A. da S. Curvelo and O. N. Oliveira Jr, *Thin Solid Films*, 1998, **327**, 47–51.
19 X. Lin, M. Zhou, S. Wang, H. Lou, D. Yang and X. Qiu, *ACS Sustainable Chem. Eng.*, 2014, **2**, 1902–1909.
20 X. Liu, H. Yin, Z. Zhang, B. Diao and J. Li, *Colloids Surf., B*, 2015, **125**, 230–237.
21 J. Yu, J. F. Wang, C. P. Wang, Y. P. Liu, Y. Z. Xu, C. B. Tang and F. X. Chu, *Macromol. Rapid Commun.*, 2015, **36**, 398.
22 Y. S. Kim and J. F. Kadla, *Biomacromolecules*, 2010, **11**, 981–988.
23 H. Liu and H. Chung, *Macromolecules*, 2016, **49**, 7246–7256.
24 D. S. Argyropoulos, H. Sadeghifar, C. Cui and S. Sen, *ACS Sustainable Chem. Eng.*, 2014, **2**, 264–271.
25 A. L. Korich, A. B. Fleming, A. R. Walker, J. Wang, C. Tang and P. M. Iovine, *Polymer*, 2012, **53**, 87–93.
26 W. O. S. Doherty, P. Mousavioun and C. M. Fellows, *Ind. Crops Prod.*, 2011, **33**, 259–276.
27 J. Ruwoldt, *Surfaces*, 2020, **3**, 622–648.
28 I. Haq, P. Mazumder and A. S. Kalamdhad, *Bioresour. Technol.*, 2020, **312**, 123636.
29 S. Bauer, H. Sorek, V. D. Mitchell, A. B. Ibáñez and D. E. Wemmer, *J. Agric. Food Chem.*, 2012, **60**, 8203–8212.
30 S. Laurichesse, L. Avérous, L. Averous and L. Avérous, *Prog. Polym. Sci.*, 2014, **39**, 1266–1290.
31 E. K. Pye and J. H. Lora, *Tappi J.*, 1991, **74**, 113–118.
32 N. Hadjichristidis, H. Iatrou, M. Pitsikalis and J. Mays, *Prog. Polym. Sci.*, 2006, **31**, 1068–1132.

33 J. Sternberg, O. Sequerth and S. Pilla, *Prog. Polym. Sci.*, 2021, **113**, 101344.
34 E. Isaac, A. Samson and O. Adeosun, *Sustainable Lignin for Carbon Fibers: Principles, Techniques, and Applications*, Springer International Publishing, Cham, 2019.
35 R. Parthasarathi, R. A. Romero, A. Redondo and S. Gnanakaran, *J. Phys. Chem. Lett.*, 2011, **2**, 2660–2666.
36 H. Liu and H. Chung, *J. Polym. Sci., Part A: Polym. Chem.*, 2017, **55**, 3515–3528.
37 H. Liu and H. Chung, *ACS Sustainable Chem. Eng.*, 2017, **5**, 9160–9168.
38 D. Uhrig and J. Mays, *Polym. Chem.*, 2011, **2**, 69–76.
39 S. M. Satti and A. A. Shah, *Lett. Appl. Microbiol.*, 2020, **70**, 413–430.
40 C. Zhu, Z. Zhang, Q. Liu, Z. Wang and J. Jin, *J. Appl. Polym. Sci.*, 2003, **90**, 982–990.
41 T. Tang, T. Moyori and A. Takasu, *Macromolecules*, 2013, **46**, 5464–5472.
42 T. Kobayashi, M. Kakimoto and Y. Imai, *Polym. J.*, 1993, **25**, 741–746.
43 E. N. Zil'berman, A. E. Kulikova and N. M. Teplyakov, *J. Polym. Sci.*, 1962, **56**, 417–423.
44 H. Feuer and R. Miller, *J. Org. Chem.*, 1959, **24**, 118–119.
45 R. Okabayashi, Y. Ohta and T. Yokozawa, *Polym. Chem.*, 2019, **10**, 4973–4979.
46 N. Cohen-Arazi, J. Katzhendler, M. Kolitz and A. J. Domb, *Macromolecules*, 2008, **41**, 7259–7263.
47 Roohi, M. R. Zaheer and M. Kuddus, *Polym. Adv. Technol.*, 2018, **29**, 30–40.
48 S. A. A. Ghavimi, M. H. Ebrahimzadeh, M. Solati-Hashjin and N. A. A. Osman, *J. Biomed. Mater. Res., Part A*, 2015, **103**, 2482–2498.
49 M. Puchalski, G. Szparaga, T. Biela, A. Gutowska, S. Sztajnowski and I. Krucińska, *Polymers*, 2018, **10**, 251.
50 D. J. A. Cameron and M. P. Shaver, *Chem. Soc. Rev.*, 2011, **40**, 1761–1776.
51 V. Lassalle and M. L. Ferreira, *Macromol. Biosci.*, 2007, **7**, 767–783.
52 C. Nakafuku and H. Yoshimura, *Polymer*, 2004, **45**, 3583–3585.
53 K. Budak, O. Sogut and U. A. Aydemir, *J. Polym. Res.*, 2020, **27**, 208.
54 Y. Xu, C. S. Kim, D. M. Saylor and D. Koo, *J. Biomed. Mater. Res., Part B*, 2017, **105**, 1692–1716.
55 M. de Geus, I. van der Meulen, B. Goderis, K. van Hecke, M. Dorschu, H. van der Werff, C. E. Koning and A. Heise, *Polym. Chem.*, 2010, **1**, 525–533.
56 H. Liu, N. Mohsin, S. Kim and H. Chung, *J. Polym. Sci., Part A: Polym. Chem.*, 2019, **57**, 2121–2130.
57 P. Karuppuswamy, J. R. Venugopal, B. Navaneethan, A. L. Laiva and S. Ramakrishna, *Mater. Lett.*, 2015, **141**, 180–186.
58 L. Cabedo, J. L. Feijoo, M. P. Villanueva, J. M. Lagarón and E. Giménez, *Macromol. Symp.*, 2006, **233**, 191–197.
59 S. Rahmani, M. Maroufkhani, S. Mohammadzadeh-Komuleh and Z. Khoubi-Arani, in *Fundamentals of Bionanomaterials*, Elsevier, 2022, pp. 175–215.
60 J. R. Dias, A. Sousa, A. Augusto, P. J. Bártolo and P. L. Granja, *Polymers*, 2022, **14**, 3397.
61 N. Mulchandani, K. Masutani, S. Kumar, S. Sakurai, Y. Kimura and V. Katiyar, *Mater. Today Commun.*, 2022, **33**, 104040.
62 A. Haryńska, J. Kucinska-Lipka, A. Sulowska, I. Gubanska, M. Kostrzewa and H. Janik, *Materials*, 2019, **12**, 887.
63 S. Müller, H. Uyama and S. Kobayashi, *Chem. Lett.*, 1999, **28**, 1317–1318.
64 A. Pascual, H. Sardon, A. Veloso, F. Ruipérez and D. Mecerreyes, *ACS Macro Lett.*, 2014, **3**, 849–853.
65 A. Pascual, H. Sardón, F. Ruipérez, R. Gracia, P. Sudam, A. Veloso and D. Mecerreyes, *J. Polym. Sci., Part A: Polym. Chem.*, 2015, **53**, 552–561.
66 W. N. Ottou, H. Sardon, D. Mecerreyes, J. Vignolle and D. Taton, *Prog. Polym. Sci.*, 2016, **56**, 64–115.
67 D. McGinty, C. S. Letizia and A. M. Api, *Food Chem. Toxicol.*, 2011, **49**, S174–S182.
68 S. Ravi, D. Padmanabhan and V. R. Mamdapur, *J. Indian Inst. Sci.*, 2013, **81**, 299.
69 J. Pais, I. Farinha, F. Freitas, L. S. Serafim, V. Martínez, J. C. Martínez, M. Arévalo-Rodríguez, M. A. Prieto and M. A. M. Reis, *Enzyme Microb. Technol.*, 2014, **55**, 151–158.
70 A. Bera, S. Dubey, K. Bhayani, D. Mondal, S. Mishra and P. K. Ghosh, *Int. J. Biol. Macromol.*, 2015, **72**, 487–494.
71 A. A. Pantazaki, C. P. Papaneophytou, A. G. Pritsa, M. Liakopoulou-Kyriakides and D. A. Kyriakidis, *Process Biochem.*, 2009, **44**, 847–853.
72 J.-H. Lin, M.-C. Lee, Y.-S. Sue, Y.-C. Liu and S.-Y. Li, *Appl. Microbiol. Biotechnol.*, 2017, **101**, 6419–6430.
73 J. Marudkla, W.-C. Lee, S. Wannawilai, Y. Chisti and S. Sirisansaneeyakul, *J. Biotechnol.*, 2018, **268**, 12–20.
74 S. J. Park, Y. Jang, W. Noh, Y. H. Oh, H. Lee, Y. David, M. G. Baylon, J. Shin, J. E. Yang and S. Y. Choi, *Biotechnol. Bioeng.*, 2015, **112**, 638–643.
75 N. Biglari, M. G. Dashti, P. Abdeshahian, I. Orita, T. Fukui and K. Sudesh, *3 Biotech*, 2018, **8**, 330.
76 A. F. M. Yatim, I. M. Syafiq, K. H. Huong, A.-A. A. Amirul, A. W. M. Effendy and K. Bhubalan, *BioTechnologia*, 2017, **2**, 141–151.
77 R. Das, N. R. Saha, A. Pal, D. Chattopadhyay and A. K. Paul, *Front. Biol.*, 2018, **13**, 297–308.
78 D. Kalaiyezhini and K. B. Ramachandran, *Prep. Biochem. Biotechnol.*, 2015, **45**, 69–83.
79 P. C. Sabapathy, S. Devaraj, A. Parthiban and P. Kathirvel, *Environ. Technol.*, 2018, **39**, 1430–1441.
80 C. F. P. Malacara, A. G. Romero, M. M. Ponce and T. C. Marenco, *Microbial Factories*, Springer, India, New Delhi, 2015.
81 J. Valdés, G. Kutralam-Muniasamy, B. Vergara-Porras, R. Marsch, F. Pérez-Guevara and M. R. López-Cuellar, *Nat. Biotechnol.*, 2018, **40**, 200–206.

82 M. C. Eremia, I. Lupescu, M. Vladu, M. Petrescu, G. Savoiu, A. Stefaniu and M. Spiridon, *Ovidius Univ. Ann. Chem.*, 2016, **27**, 44–47.
83 J. Fernández, H. Amestoy, H. Sardon, M. Aguirre, A. L. Varga and J. R. Sarasua, *J. Mech. Behav. Biomed. Mater.*, 2016, **64**, 209–219.
84 S. Tiptipakorn, N. Keungputpong, S. Phothiphiphit and S. Rimdusit, *J. Appl. Polym. Sci.*, 2015, **132**(18), 41915.
85 J. Fernández, H. Amestoy, H. Sardon, M. Aguirre, A. L. Varga and J.-R. Sarasua, *J. Mech. Behav. Biomed. Mater.*, 2016, **64**, 209–219.
86 J. Fernández, M. Montero, A. Etxeberria and J.-R. Sarasua, *Polym. Degrad. Stab.*, 2017, **137**, 23–34.
87 G. Cama, D. E. Mogosanu, A. Houben and P. Dubruel, in *Science and Principles of Biodegradable and Bioresorbable Medical Polymers*, Elsevier, 2017, pp. 79–105.
88 Z. Luo, Y. L. Wu, Z. Li and X. J. Loh, *Biotechnol. J.*, 2019, **14**, 1900283.
89 K. Sudesh, H. Abe and Y. Doi, *Prog. Polym. Sci.*, 2000, **25**, 1503–1555.
90 M. Koller, *Bioengineering*, 2019, **6**, 34.
91 Z. A. Raza, S. Noor and S. Khalil, *Biotechnol. Prog.*, 2019, **35**, e2855.
92 A. V. Samrot, S. K. Samanvitha, N. Shobana, E. R. Renitta, P. Senthilkumar, S. S. Kumar, S. Abirami, S. Dhiva, M. Bavanilatha, P. Prakash, S. Saigeetha, K. S. Shree and R. Thirumurugan, *Polymers*, 2021, **13**, 3302.
93 Q. Gao, H. Yang, C. Wang, X.-Y. Xie, K.-X. Liu, Y. Lin, S.-Y. Han, M. Zhu, M. Neureiter, Y. Lin and J.-W. Ye, *Front. Bioeng. Biotechnol.*, 2022, **10**, 966598.
94 J. Rydz, W. Sikorska, M. Kyulavska and D. Christova, *Int. J. Mol. Sci.*, 2015, **16**, 564–596.
95 S. R. Andersson, M. Hakkarainen, S. Inkinen, A. Södergård and A.-C. Albertsson, *Biomacromolecules*, 2010, **11**, 1067–1073.
96 A. A. Shah, S. Kato, N. Shintani, N. R. Kamini and T. Nakajima-Kambe, *Appl. Microbiol. Biotechnol.*, 2014, **98**, 3437–3447.
97 R.-J. Müller, I. Kleeberg and W.-D. Deckwer, *J. Biotechnol.*, 2001, **86**, 87–95.
98 M. S. Kim, H. Chang, L. Zheng, Q. Yan, B. F. Pfleger, J. Klier, K. Nelson, E. L.-W. Majumder and G. W. Huber, *Chem. Rev.*, 2023, **123**, 9915–9939.
99 T. Hiraishi and S. Taguchi, *Mini-Rev. Org. Chem.*, 2009, **6**, 44–54.
100 A. Banerjee, K. Chatterjee and G. Madras, *Mater. Sci. Technol.*, 2014, **30**, 567–573.
101 S.-J. Zhou, H.-M. Wang, S.-J. Xiong, J.-M. Sun, Y.-Y. Wang, S. Yu, Z. Sun, J.-L. Wen and T.-Q. Yuan, *ACS Sustainable Chem. Eng.*, 2021, **9**, 12017–12042.
102 Y. L. Chung, J. V. Olsson, R. J. Li, C. W. Frank, R. M. Waymouth, S. L. Billington and E. S. Sattely, *ACS Sustainable Chem. Eng.*, 2013, **1**, 1231–1238.
103 L. Dai, Q. Cao, K. Wang, S. Han, C. Si, D. Liu and Y. Liu, *Ind. Crops Prod.*, 2020, **143**, 111954.
104 R. Liu, L. Dai, Z. Zou and C. Si, *Int. J. Biol. Macromol.*, 2018, **119**, 1129–1136.
105 W. Ren, X. Pan, G. Wang, W. Cheng and Y. Liu, *Green Chem.*, 2016, **18**, 5008–5014.
106 L. E. Chile, S. J. Kaser, S. G. Hatzikiriakos and P. Mehrkhodavandi, *ACS Sustainable Chem. Eng.*, 2018, **6**, 1650–1661.
107 M. Gallego-García, A. D. Moreno, P. Manzanares, M. J. Negro and A. Duque, *Bioresour. Technol.*, 2023, **369**, 128397.
108 S. P. Makri, E. Xanthopoulou, M. A. Valera, A. Mangas, G. Marra, V. Ruiz, S. Koltsakidis, D. Tzetzis, A. Z. Karathanasis, I. Deligkiozi, N. Nikolaidis, D. Bikiaris and Z. Terzopoulou, *Polymers*, 2023, **15**, 2386.
109 S. P. Makri, P. A. Klonos, G. Marra, A. Z. Karathanasis, I. Deligkiozi, M. Á. Valera, A. Mangas, N. Nikolaidis, Z. Terzopoulou, A. Kyritsis and D. N. Bikiaris, *Soft Matter*, 2024, **20**, 5014–5027.
110 S. Y. Park, J. Y. Kim, H. J. Youn and J. W. Choi, *Int. J. Biol. Macromol.*, 2019, **138**, 1029–1034.
111 Q. Zong, A. Xu, K. Chai, Y. Zhang and Y. Song, *Polym. Adv. Technol.*, 2020, **31**, 2239–2249.
112 R. Liu, L. Dai, L.-Q. Hu, W.-Q. Zhou and C.-L. Si, *Mater. Sci. Eng., C*, 2017, **80**, 397–403.
113 X.-F. Wei, R.-Y. Bao, Z.-Q. Cao, W. Yang, B.-H. Xie and M.-B. Yang, *Macromolecules*, 2014, **47**, 1439–1448.
114 M. Li, Y. Pu, F. Chen and A. J. Ragauskas, *Nat. Biotechnol.*, 2021, **60**, 189–199.
115 R. A. Pérez-Camargo, G. Saenz, S. Laurichesse, M. T. Casas, J. Puiggalí, L. Avérous and A. J. Müller, *J. Polym. Sci., Part B: Polym. Phys.*, 2015, **53**, 1736–1750.
116 M. Abdollahi, R. B. Habashi and M. Mohsenpour, *Ind. Crops Prod.*, 2019, **130**, 547–557.
117 S. Laurichesse and L. Avérous, *Polymer*, 2013, **54**, 3882–3890.
118 J. Wang, L. Tian, B. Luo, S. Ramakrishna, D. Kai, X. J. Loh, I. H. Yang, G. R. Deen and X. Mo, *Colloids Surf., B*, 2018, **169**, 356–365.
119 I.-K. Park, H. Sun, S.-H. Kim, Y. Kim, G. E. Kim, Y. Lee, T. Kim, H. R. Choi, J. Suhr and J.-D. Nam, *Sci. Rep.*, 2019, **9**, 7033.
120 A. Duda, S. Penczek, A. Kowalski and J. Libiszowski, *Macromol. Symp.*, 2000, **153**, 41–53.
121 A. Kowalski, A. Duda and S. Penczek, *Macromolecules*, 2000, **33**, 689–695.
122 M. Ryner, K. Stridsberg, A. C. Albertsson, H. Von Schenck and M. Svensson, *Macromolecules*, 2001, **34**, 3877–3881.
123 W. Punyodom, W. Limwanich, P. Meepowpan and B. Thapsukhon, *Des. Monomers Polym.*, 2021, **24**, 89–97.
124 M. C. Najarro, M. Nikolic, J. Iruthayaraj and I. Johannsen, *ACS Appl. Polym. Mater.*, 2020, **2**, 5767–5778.
125 Y. Zhang, J. Liao, X. Fang, F. Bai, K. Qiao and L. Wang, *ACS Sustainable Chem. Eng.*, 2017, **5**, 4276–4284.
126 J. Tian, Y. Yang and J. Song, *Int. J. Biol. Macromol.*, 2019, **141**, 919–926.
127 J. J. C. Lee, S. Sugiarto, P. J. Ong, X. Y. D. Soo, X. Ni, P. Luo, Y. Y. K. Hnin, J. S. Y. See, F. Wei, R. Zheng,

P. Wang, J. Xu, X. J. Loh, D. Kai and Q. Zhu, *J. Energy Storage*, 2022, **56**, 106118.
128 D. Xie, Y. Pu, X. Meng, N. D. Bryant, K. Zhang, W. Wang, A. J. Ragauskas and M. Li, *ACS Sustainable Chem. Eng.*, 2022, **10**, 16882–16895.
129 S. H. Jang, D. H. Kim, D. H. Park, O. Y. Kim and S. H. Hwang, *Prog. Org. Coat.*, 2018, **120**, 234–239.
130 A. Lendlein, A. M. Schmidt and R. Langer, *Proc. Natl. Acad. Sci. U. S. A.*, 2001, **98**, 842–847.
131 P. Deshmukh, H. Yoon, S. Cho, S. Y. Yoon, O. V. Zore, T. Kim, I. Chung, S. Ahn and R. M. Kasi, *J. Polym. Sci., Part A: Polym. Chem.*, 2017, **55**, 3424–3433.
132 Q. Zhao, W. Zou, Y. Luo and T. Xie, *Sci. Adv.*, 2016, **2**, e1501297.
133 Q. Zhao, H. J. Qi and T. Xie, *Prog. Polym. Sci.*, 2015, **49**, 79–120.
134 S. Kim and H. Chung, *ACS Sustainable Chem. Eng.*, 2021, **9**, 14766–14776.
135 B. McAdam, M. B. Fournet, P. McDonald and M. Mojicevic, *Polymers*, 2020, **12**, 2908.
136 I. Vroman and L. Tighzert, *Materials*, 2009, **2**, 307–344.
137 F. M. García-Valle, V. Tabernero, T. Cuenca, M. E. G. Mosquera, J. Cano and S. Milione, *Organometallics*, 2018, **37**, 837–840.
138 S. M. Guillaume, L. Annunziata, I. del Rosal, C. Iftner, L. Maron, P. W. Roesky and M. Schmid, *Polym. Chem.*, 2013, **4**, 3077–3087.
139 J. Dobrogojski, M. Spychalski, R. Luciński and S. Borek, *Acta Physiol. Plant.*, 2018, **40**, 1–17.
140 R. Handrick, S. Reinhardt, P. Kimmig and D. Jendrossek, *J. Bacteriol.*, 2004, **186**, 7243–7253.
141 D. Kai, K. Zhang, S. S. Liow and X. J. Loh, *ACS Appl. Bio Mater.*, 2019, **2**, 127–134.
142 Y. Sun, L. Yang, X. Lu and C. He, *J. Mater. Chem. A*, 2015, **3**, 3699–3709.
143 D. Kai, K. Zhang, L. Jiang, H. Z. Wong, Z. Li, Z. Zhang and X. J. Loh, *ACS Sustainable Chem. Eng.*, 2017, **5**, 6016–6025.
144 W. Yang, G. Qi, H. Ding, P. Xu, W. Dong, X. Zhu, T. Zheng and P. Ma, *Compos. Commun.*, 2020, **22**, 100497.
145 A. L. Rivera-Briso and Á. Serrano-Aroca, *Polymers*, 2018, **10**(7), 732.
146 M. Larsson, O. Markbo and P. Jannasch, *RSC Adv.*, 2016, **6**, 44354–44363.
147 Y.-X. Weng, Y. Wang, X.-L. Wang and Y.-Z. Wang, *Polym. Test.*, 2010, **29**, 579–587.
148 E. Bugnicourt, P. Cinelli, A. Lazzeri and V. Alvarez, *eXPRESS Polym. Lett.*, 2014, **8**, 791–808.
149 T. Erceg, S. Rackov and P. Terek, *Polymers*, 2023, **15**, 4694.
150 T. Ahmed, H. Marçal, M. Lawless, N. S. Wanandy, A. Chiu and L. J. R. Foster, *Biomacromolecules*, 2010, **11**, 2707–2715.
151 B. M. P. Ferreira and E. A. R. Duek, *J. Appl. Biomater. Biomech.*, 2005, **3**, 50–60.
152 M. L. Tebaldi, A. L. C. Maia, F. Poletto, F. V. de Andrade and D. C. F. Soares, *J. Drug Delivery Sci. Technol.*, 2019, **51**, 115–126.
153 F. Türesin, I. Gürsel and V. Hasirci, *J. Biomater. Sci., Polym. Ed.*, 2001, **12**, 195–207.
154 M. L. Tebaldi, A. L. C. Maia, F. Poletto, F. V. de Andrade and D. C. F. Soares, *J. Drug Delivery Sci. Technol.*, 2019, **51**, 115–126.
155 S. Luo, J. Cao and A. G. McDonald, *ACS Sustainable Chem. Eng.*, 2016, **4**, 3465–3476.
156 D. Kai, H. M. Chong, L. P. Chow, L. Jiang, Q. Lin, K. Zhang, H. Zhang, Z. Zhang and X. J. Loh, *Compos. Sci. Technol.*, 2018, **158**, 26–33.
157 E. L. Young and A. G. McDonald, *Molecules*, 2021, **26**, 2437.
158 L. Dessbesell, M. Paleologou, M. Leitch, R. Pulkki and C. (C) Xu, *Renewable Sustainable Energy Rev.*, 2020, **123**, 109768.
159 J. Kautto, M. J. Realff, A. J. Ragauskas and T. Kässi, *BioResources*, 2014, **9**, 6041–6072.
160 D. S. Bajwa, G. Pourhashem, A. H. Ullah and S. G. Bajwa, *Ind. Crops Prod.*, 2019, **139**, 111526.
161 H. Ludmila, J. Michal, Š. Andrea and H. Aleš, *Wood Res.*, 2015, **60**, 973–986.
162 Y. Han, L. Yuan, G. Li, L. Huang, T. Qin, F. Chu and C. Tang, *Polymer*, 2016, **83**, 92–100.